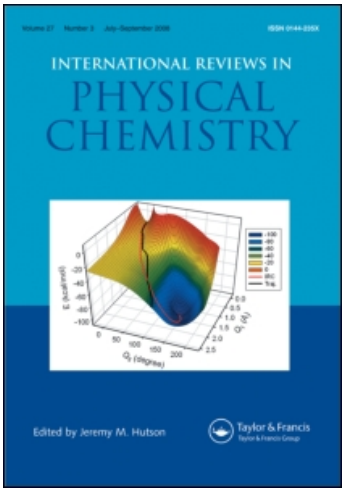

International Reviews in Physical Chemistry
Publication details, including instructions for authors and subscription information:
http://www.informaworld.com/smpp/title~content=t713724383

Kinetics and dynamics of reactions in liquids

M. Ben-Nun[a]; R. D. Levine[b]
[a] The Fritz Haber Research Center for Molecular Dynamics, The Hebrew University, Jerusalem, Israel [b] The Department of Chemistry and Biochemistry, University of California, Los Angeles, CA, USA

To cite this Article Ben-Nun, M. and Levine, R. D.(1995) 'Kinetics and dynamics of reactions in liquids', International Reviews in Physical Chemistry, 14: 2, 215 — 270
To link to this Article: DOI: 10.1080/01442359509353310
URL: http://dx.doi.org/10.1080/01442359509353310

INTERNATIONAL REVIEWS IN PHYSICAL CHEMISTRY, 1995, VOL. 14, NO. 2, 215–270

Kinetics and dynamics of reactions in liquids

by M. BEN-NUN and R. D. LEVINE
The Fritz Haber Research Center for Molecular Dynamics,
The Hebrew University, Jerusalem 91904, Israel
and The Department of Chemistry and Biochemistry,
University of California, Los Angeles,
Los Angeles, CA 90024, USA

We discuss the control of the kinetics and dynamics of chemical reactions by the solvent, from a molecular point of view. The kinetics are discussed using a transition state theory (TST) approach, applied to the reactants and their surrounding solvent as one supramolecule. The topics discussed include a molecular interpretation for the changes that take place when one solvent is being replaced by another; the use of local against normal vibrational modes and/or joint description, i.e., local modes for part of the system and normal modes for the other part; and the effect of pressure on the rate in solution. The notion of free volume and volume of activation is extended to a more general phase space in which geometrical volumes may overlap, the approximations that are inherent to cell theory are examined and a molecular interpretation for internal and chemical pressures is suggested. The link to the dynamics is provided by an analysis of the breakdown of TST due to diffusion/cage control of the rate of the reaction. A unified description which interpolates from activation control to diffusion control is presented with a special emphasis on the motion within the solvation cage. Results of molecular dynamics simulations for both activated and activationless reactions are presented. The very detailed computer experiment is interpreted using a reduced mechanical description and the separation of time-scales is discussed using an adiabatic separation of variables. Spectroscopic methods for probing the different time epochs are suggested. The rather short duration typical of the motion within the solvent cage is emphasized, and the possibilities that this affords for studying the short-time dynamical role of the solvent via experiments in clusters or in glasses are noted.

1. Introduction

Chemists influence the rates of chemical reactions in solution by changing the properties of the solvent. In this review we discuss the molecular level interpretation of the possible changes that can be brought about in this way. We consider also the role of the solvent during the entire course of the reaction because our final aim is an interpretation not only of the overall reaction rate but also the dynamics of the reaction and the ways that the solvent can intervene to modify them.

Modern chemical physics speaks of control of chemical reactions. Theoretical proposals for achieving this control are typically discussed through the application of a tailored intense laser pulse. The externally imposed laser field needs to be strong so that it can modify the forces that act between the atoms. Equally strong (and, often, chemically more specific) perturbations on the reactants are, however, possible by changing the solvent. Indeed, the perturbation by the solvent is strong enough that it is useful, as we do below, to think of the solute and the solvent together as one large supramolecule. The very specificity of the perturbation does however mean that one has to know, in some detail, the nature of the relevant regions of the potential energy

0144–235X/95 $10·00

surface of the entire system. Since this is often not realistic, chemists have given special attention to the reaction coordinate along which the system evolves en route from reactants to products. In solution the motion of the reactive system along the reaction path is coupled also to the solvent degrees of freedom. If one is willing to view the reactive system immersed in a liquid as a supramolecule, this coupling will be additional to the coupling between the reaction coordinate and the degrees of freedom of the isolated reactants. In this review we will often adopt a gas phase view on chemical dynamics in solution. By doing so we can apply, to some extent, the accumulated understanding of gas phase reaction dynamics to reactions in solution.

In the gas phase, the rate of a thermally activated bimolecular chemical reaction is given, using transition state theory (TST), by the rate of crossing the barrier to reaction. This crossing may no longer be the rate determining step for reactions in solution as the liquid may hinder the approach motion of the reactants. The observed net reaction rate is then limited by two processes: the diffusion of the two reactants into a mutual solvation shell and the barrier crossing event. In this review we centre attention on the second process, i.e., the crossing of the chemical barrier to reaction, but we do comment on how one could account, in a Rice–Ramsperger–Kassel–Marcus (RRKM) type fashion, for the presence of both a solvent barrier and a chemical barrier to reaction. We further show how a unified point of view can interpolate between a diffusion limited and a chemical barrier limited rate of reaction. On the other hand, it should be emphasized that the chemical barrier may well involve the participation of the solvent degrees of freedom and is by no means necessarily the same as the barrier to reaction in the gas phase.

As has been often noted, transition state theory can be written in a way that is exact. In other words, there does exist a distribution of states known as the distribution of reactive reactants such that the flux through the barrier, averaged over this distribution is the exact rate of reaction. In this review we use the much more practical, but approximate, version of the theory which says that this distribution is the equilibrium distribution of states at the barrier. The actual implementation of this prescription can be carried out in one of two ways. The first approach involves thermodynamic properties such as free energy, enthalpy, entropy and volume of activation. These are often measurable properties and thus experimentalists will often use the thermodynamic formulation. The second, statistical mechanics approach is formulated using the molecular properties of the system and it is somewhat more dynamically oriented. It requires a knowledge of the potential energy of the entire system (i.e., reactants plus solvent) in the immediate vicinity of the surface dividing the reactants from the products, and it involves the calculation of partition functions. Reconciling these two points of view is one objective of the first part of this review. In particular, an attempt will be made to give a molecular interpretation to such heuristic thermodynamic properties as internal pressure or free volume. We do so by formulating the transition state theory expression in different ways and choosing the one that is most useful for our needs.

The starting point for any subsequent approximation that we will make is the exact classical statistical mechanics expression for the transition state rate constant as a ratio between two phase space integrals: one at the transition state and one for the reactants. The essential point and one that we will repeatedly invoke is that, in classical mechanics, a thermal average can be considered as a double average: one over the momentum variables and one over the space variables. It follows that one can factor any partition function as a product of a momentum integral and a configuration integral. While this

is well known in statistical mechanics, it is not often applied in chemical kinetics (with the very notable exception of Johnston's (1966) book). Presumably, the reason is that such a factorization has no immediate thermodynamic analog. However, since the surface of no return, that defines the transition state, is usually taken to be momentum independent, the integral over phase space at the transition state configuration can also be factored into an integral over momentum and over position. There is therefore no reason not to apply this factorization in chemical kinetics and we shall invoke it, repeatedly, below.

It is the integral over the coordinates, often called the configurational integral, which requires the multi-dimensional potential energy surface as an input. Depending on the degree of coupling between the different coordinates the calculation of the configurational integral will be more or less complicated. In any event one has to remember that the very same input is required also for the more familiar route of evaluation of the partition function through the energy levels. We shall also show that the two configurational integrals that are needed for the rate constant can be expressed in terms of the, so called, potential of mean force (PMF) at the transition state and for the reactants, respectively.

The result of the configuration and momentum integrals does not depend on the particular choice of a coordinate system and one can use different coordinate systems at the transition state and for the reactants and/or for momenta and positions. Different choices of coordinate systems will be shown to result in different expressions for the rate constant and in particular we will discuss when one should use local or normal coordinates and what approximations are applicable for each of these choices. Local mode properties have been used by Johnston (1966) to express the gas phase transition state rate constant. Here we extend this formalism to the liquid phase with the same basic motivation. Any rate constant that involves a complicated large molecule will require the evaluation of many vibrational amplitudes. When the system evolves along the reaction coordinate many of these vibrational amplitudes may hardly change and thus cancel identically without ever having to be computed. In solution this may greatly simplify the problem as most of the local (and sometimes even normal) properties will involve only the pure solvent degrees of freedom. Since the solvation of any species, even ionic, is largely due to the first solvation shell, the assumption that most of these local properties will cancel out is not unreasonable.

When possible connection will be made between the present discussion and other dynamical theories, such as the familiar Grote–Hynes expression (1980) for the TST rate constant in solution. Different approximations will be examined for the following reasons. We wish to see what are the approximations that are needed in order to relate the statistical mechanics expression to such thermodynamic properties as free volume and internal pressure. Furthermore, we would like to examine the possibility of a reduced description of liquid phase dynamics (below we explain in detail why). The analysis of the rate constant expression enables us to directly indicate to the reader which coordinates are neglected in the reduced description and which are included.

To be really able to control liquid phase chemical reactions one needs to go beyond statistical theories and reveal the complete time history of the system as it evolves along the reaction coordinate. The reason why we need to go beyond TST is quite obvious if we want to determine the role of the solvent in activating (deactivating) the reactants (products), or if we wish to understand (on a molecular level) how the solvent impedes the products as they separate. This last phenomenon is known as the traditional cage effect (Frank and Rabinowitch 1934, North 1964) and it has been extensively studied

by computer simulations (Whitnell and Wilson 1993). Thus the second part of this review will discuss dynamics and in particular a reduced dynamical description. Superficially it may look as if there is no need for such a reduced description as the available computer power enables us to monitor the time evolution of both the reactive system and the solvent molecules at relative ease. The human mind, on the other hand, is more limited and the output from the simulations is often too large. Hence, the use of a reduced description of the many-body problem is motivated by two different reasons: one has to do with the fact that often one is interested in a small subset of the system, the reactants, and the properties of the solvent are of no interest, yet much of the computation time is spent on calculating the solvent properties. The second reason is, the above mentioned, over abundance of data which is often too detailed for our needs. We therefore view the molecular dynamics simulations as a very detailed experiment that calls for an interpretation.

The reduced mechanical approach which we discuss below is by no means the only way of reducing the complexity of the problem. Another, widely used, description is based on modelling the solvent using two terms: one is a dissipative term, proportional to the velocity, which mimics the dissipation of momentum of the reactants to the solvent degrees of freedom and the second is a random force. The latter describes collisions with the solvent that activate (or deactivate) the reactants. (The two terms are related by the second fluctuation–dissipation theorem and thus ensure the final long-time thermal equilibration of the system.) The distinction between the two terms is phenomenological and the resulting Langevin equation, or generalized Langevin equation (GLE) for the case when memory effects are incorporated, is but an approximation. It is generally agreed that if the potential along the reaction coordinate and the magnitude (and shape) of the friction are correctly modelled, trends and systematics of an ensemble of full classical molecular dynamics trajectories are correctly predicted by an ensemble of stochastic trajectories at a much lower (typically two orders of magnitude) computational cost.

We conclude this introduction (Eco 1994) by listing reviews and collections which complement and supplement our discussion. These include Adelman (1983, 1987), Agmon and Levine (1994), Berne *et al.* (1988), Burshtein and Kivelson (1991), Chandler (1990), Fonesca *et al.* (1985), Hänggi *et al.* (1990), Hänggi and Troe (1991), Harris *et al.* (1988), Hynes (1985a, b), Jortner *et al.* (1993), Melnikov (1991), Nitzan (1988), Robinson *et al.* (1990), Schroeder and Troe (1987), Truhlar (1990), Tucker *et al.* (1991), Whitnell and Wilson (1993), Wilson (1988a), Zhang and Harris (1991).

2. Prelude: The supramolecular partition function

The transition state theory expression for the rate constant

$$k(T) = \frac{kT}{h}\frac{Q^{\ddagger}}{Q^{r}}\exp(-\Delta E/k_{B}T) \tag{1}$$

is well known (Berne *et al.* 1988, Glasstone *et al.* 1944, Truhlar 1990). In the classical limit this requires the calculation of phase integrals at the TS ($Q^{\ddagger}$) and for the reactants (Q^{r}) and knowledge of ΔE, the energy difference between the TS and the reactants. It is generally assumed that neither the potential nor the transition state dividing surface depend on the momenta so that the classical phase integral can be factorized into a product of integrals over momenta and positions. The latter is the configurational

integral over the Boltzmann factor of the potential energy

$$Z = \int \ldots \int \exp\left[-u(\mathbf{x})/k_B T\right] \mathrm{d}x_1 \ldots \mathrm{d}x_{3N}. \tag{2}$$

The purpose of this section is to discuss the approximations available for the evaluation of this integral with special reference to the point of view where we consider the reactants and the surrounding solvent as one supramolecule. We do however want to make contact with the rate of the corresponding gas phase reaction, on the one hand, and the properties of the solvent on the other. For this purpose it proves convenient to distinguish at least three sets of degrees of freedom that are needed to specify a configuration of the supramolecule: those of the isolated (gas phase) reactants, those of the solvent and those that specify the relative solute–solvent configuration. The pure solvent degrees of freedom will, in general, include both the internal coordinates of the solvent molecule and the relative positions of the molecules of the solvent.

Formally, the configurational integral can always be written as a product of volume elements, V_α, available to the atoms of the molecule (Mayer and Mayer 1940)

$$Z = \prod_N V_\alpha. \tag{3}$$

If there were no forces between the atoms, each atom would move independently throughout the volume, V, of the container so that $V_\alpha = V$. In a molecule (or in our supramolecule), the atoms are not free to move independently and each atom would have an effective volume, V_α, in which it can move. This idea of an effective volume that is available to an atom is closely related to the concept of free volume that is often used in cell theory of liquids and crystals (Eyring *et al.* 1936, Fowler and Guggenhiem 1939, Hirschfelder *et al.* 1954, Hill 1987). The technical purpose of this section is to review the possible approximations for evaluating the volumes V_α. Of course, different approximations will be needed for say an atom of the reactants against an atom of a monoatomic solvent. The latter is the simplest case and we start from it.

2.1. *The free volume*

Physically the idea of free volume is quite clear. Imagine a simple monoatomic solvent and suppose that one atom is designated as being special. We focus our attention on this special atom and define the free volume to be that space in which the centre of the atom can move and still not collide (on the average) with the neighbouring atoms. The extension to a molecular solvent is straightforward. Cell theory gives a more rigorous mathematical definition of the free volume (Kirkwood 1950). If we consider a one-component, monoatomic, classical system of N particles we can divide the volume V into an imaginary lattice of N cells $\Delta_1, \Delta_2 \ldots \Delta_N$ each of volume $\vartheta = V/N$. The free volume can be shown to be related to the configurational entropy per molecule, $S^{(1)}$, in a system restrained by a single occupancy of cells

$$\begin{aligned} S^{(1)} &= Nk_B \ln \vartheta_f, \quad \vartheta_f \equiv \text{free volume}, \\ S^{(1)} &= -k_B T \int_{\Delta_1} \ldots \int_{\Delta_N} p \ln p \, \mathrm{d}\mathbf{r}_1 \ldots \mathrm{d}\mathbf{r}_N, \end{aligned} \tag{4}$$

where p is the probability of finding particle 1 in $\mathrm{d}\mathbf{r}_1$ at $\mathbf{r}_1$, 2 in $\mathrm{d}\mathbf{r}_2$ at $\mathbf{r}_2$ etc. (Bold letters are used throughout the manuscript to designate matrices and/or vectors.)

The value of the free volume itself may be estimated in different ways. The most obvious, but not so informative, procedure is to calculate the ideal free volume,

i.e. assuming no interactions and point particles, and then subtracting from it the volume that is taken by the particles. As a first crude approximation one can use a hard-sphere model to approximate this excluded volume (Eyring and Hirschfelder 1937, Hirschfelder 1939). A better approximation is given by calculating the distance of closest approach at a given temperature using a pair-wise potential to describe the interaction between the two colliding particles (Hirschfelder *et al.* 1937). An even better estimation for the free volume is attained by recognizing that the molecule does not move freely around its cell since it interacts with all of its nearest neighbours (Fowler and Guggenheim 1939). The effective free volume available for the molecule is then defined by the equation

$$\vartheta_f = \int_{\Delta} \exp\{-[\phi(\mathbf{r}) - \phi(0)]/k_B T\}\, d\mathbf{r}. \tag{5}$$

where Δ is again the volume of the cell, $\phi(\mathbf{r})$ is the total interaction of the central atom with all of its nearest neighbours when the central atom is at a distance $\mathbf{r}$ from its lattice site. This total interaction is given by a single pair-wise interaction times the number of nearest neighbours smeared on an area of a ring on the sphere of the cell. To simplify the problem the cell may be assumed to be spherical and the nearest neighbours are treated as uniformly distributed on this spherical sphere.

This last definition of the classical free volume is nothing but a mean field approximation for each particle that is confined to move in a certain cell under the influence of an averaged potential that is induced by the neighbouring atoms. It is also a continuous geometrical theory in that the integrals are over true geometrical cells that cannot overlap. In the exact derivation of the transition state theory expression for the rate constant in solution we would use a more general definition for the free or effective volume. It will involve integrals over cells in a phase space that is not necessarily geometrical so that different cells may overlap. The reason why we need to appeal for this more general definition is clear if we note that if we assume that the central molecule interacts with its neighbouring atoms via a harmonic potential the integral used for the estimation of the free volume, equation (5), reduces to the configurational part of the classical three-dimensional vibrational partition function. The resulting vibrational amplitude is local in the sense that it is confined to a region in space. This will no longer be true if the integrals involve some normal and not local modes.

2.2. *Local coordinates in solution*

The rate constant, equation (1), is expressed as a ratio of partition functions. These may have many atoms or groups of atoms whose free volume is essentially the same at the reactants and in the transition state configuration. The contribution of such terms will cancel and this greatly reduces the complexity of the calculation of the rate. The use of local coordinates serves to simplify the identification of those contributions that will cancel.

The form of the partition function that we seek should depend on local properties that are determined to a large extent by the bonds in the vicinity of each atom. The derivation does not involve any approximations beyond those assumed in the usual derivations, i.e. anharmonicity and coupling between vibration and rotation are neglected.

The formal partitioning of the configurational integral to a product of volume elements, is our starting point and we follow the derivation of Johnston (Herschbach *et al.* 1959, Johnston 1966). In our large molecule with N atoms (N typically being a

very large number as it includes all the solvent atoms) the first atom may be regarded as free to move around the whole volume with the other atoms keeping their distances rigidly with respect to it (Mayer and Mayer 1940). The evaluation of the configuration integral is thereby reduced to evaluating the effective volume terms for each atom in terms of the potential energy parameters and bond lengths and angles that relate each atom to its neighbours in the molecule. To show how this is done we first evaluate the classical partition function in the more familiar way. The configuration of the molecule is then expressed in terms of the centre of mass coordinates, the Eulerian angles that specify the orientation of the principal axes of inertia with respect to the whole molecule and the normal vibrational coordinates (Mayer and Mayer 1940, Wilson *et al.* 1955). If we assume that the rotations and vibrations are not coupled and neglect anharmonic vibrational terms the molecular energy is separable and the result for the classical partition function has the well known form

$$Q_{\text{class}} = V 8\pi^2 (2\pi k_B T/h^2)^3 M^{3/2} |\mathbf{I}|^{1/2} \prod_{i=1}^{3N-6} \frac{k_B T}{h\nu_i}. \tag{6}$$

In equation (6) V is the volume of the container, M is the molecular mass, i.e. the sum of solute and solvent masses, $|\mathbf{I}|$ is the determinant of the moment of inertia tensor and ν_i is the ith normal mode vibrational frequency. We now compare this expression to the one written in terms of the de Brogie wavelength of each particle

$$\Lambda_\alpha = h/(2\pi m_\alpha k_B T)^{1/2}. \tag{7}$$

The form for the partition function in terms of the configuration integral is derived by integrating only over the momentum of each particle in the system

$$Q_{\text{class}} = Z \prod_{\alpha=1}^{N} \Lambda_\alpha^{-3}. \tag{8}$$

By comparing (6) and (8), the configurational integral, Z, is given by

$$Z = V 8\pi^2 (2\pi k_B T/h^2)^{-1/2(3N-6)} M^{3/2} |\mathbf{I}|^{1/2} \prod_{\alpha=1}^{N} m_\alpha^{-1} \prod_{i=1}^{3N-6} \frac{k_B T}{h\nu_i}. \tag{9}$$

This last result expresses the configurational integral in terms of the normal modes of the system. As the goal is to write it in terms of local properties, we make use of the known relation between the product of the eigenvalues of the normal modes and the determinants of the $(3N-6) \times (3N-6)$ **F** and **G** matrices (Wilson *et al.* 1955). (These are the non-diagonal matrices that appear in the expression for the vibrational energy written in terms of internal coordinates. The **F** matrix is a force constants matrix and **G** is a mass matrix.)

$$|\mathbf{F}||\mathbf{G}| = \prod_{i=1}^{3N-6} \lambda_i, \tag{10}$$

where $\lambda_i = (2\pi\nu_i)^2$. Using this relation and rearranging terms the final result can be written in terms of a geometrical factor, J, times a function of the determinant of the force constants matrix times a function of the temperature

$$Z = J/(2\pi k_B T/h^2)^{1/2(3N-6)} |\mathbf{F}|^{-1/2}. \tag{11}$$

The geometrical factor J,

$$J = V 8\pi^2 M^{3/2} |\mathbf{I}|^{1/2} |\mathbf{G}|^{-1/2} \prod_{\alpha=1}^{N} m_\alpha^{-3/2} \tag{12}$$

can be shown to depend only on the geometry of the system and it can be written as a product of factors, one for each atom (Johnston 1966).

In our formulation of the transition state rate constant we use equation (11) with a single modification. Because the partition function for the transition state does not include an integration over the reaction coordinate we multiply and divide by the frequency of crossing of the transition state, ν^*. We note that in solution, this frequency need not be identical to the one in the gas phase as the crossing of the transition state will, in general, involve also the motion of the solvent. Thus the general expression for the transition state rate constant in solution is written in terms of ratios between different determinants times a frequency factor times an exponential energy factor

$$k(T) = \nu^* \left(\frac{|\mathbf{I}^{\ddagger}|^{1/2}}{|\mathbf{I}^{r}|^{1/2}}\right)\left(\frac{|\mathbf{G}^{\ddagger}|^{-1/2}}{|\mathbf{G}^{r}|^{-1/2}}\right)\left(\frac{|\mathbf{F}^{\ddagger}|^{-1/2}}{|\mathbf{F}^{r}|^{-1/2}}\right) \exp(-\Delta E/k_B T). \tag{13}$$

Here the superscript ‡(r) refers to the transition state (reactants), and ΔE is the difference in energy between the activated complex and the reactants in solution.

Equation (13) is exact within the limitations of transition state theory and the two approximations made in its derivation: a local quadratic approximation for the potential and the neglect of coupling between rotation and vibration.

We now proceed in the analysis of the expression for the transition state rate constant. We wish to note and emphasize that the analysis is performed simultaneously on both the **F** and **G** matrices. This enables us to identify eigenvalues of the product of these matrices with normal modes of vibration. The desired final forms would either relate the microscopic properties of the rate constant (that are derived in terms of the form of a molecular Hamiltonian), or to thermodynamic quantities, or be written as a gas phase rate constant times a liquid phase correction factor. Depending on the solvent, and on the potential along the reaction coordinate in the region of the transition state and of the reactants this correction term would be of smaller or larger magnitude.

To enable the reader to follow the formulation in a most convenient way we define the following matrices that would often show up in what follows.

$$\mathbf{FG} = \begin{pmatrix} \mathbf{A} & \mathbf{W}^{T} \\ \mathbf{W} & \mathbf{B} \end{pmatrix} \text{ and } \mathbf{A} = \begin{pmatrix} \mathbf{S} & \mathbf{C}^{T} \\ \mathbf{C} & \mathbf{K} \end{pmatrix}. \tag{14}$$

The non-diagonal matrix **S** correspond to the solute internal modes, **K** describes the solvent–solute relative separation and **C** is the coupling between these two sets of modes. The second non-diagonal matrix, **B**, represents the pure solvent degrees of freedom, and these are coupled to all the other modes via the matrix **W**. The matrices, **K**, **S**, **B** and **A** are square matrices and in general **B** would be the largest one as it includes all the solvent–solvent internal coordinates.

In the next sections we examine different possible analytical forms of the rate constant. Use will often be made of a mathematical result (Hohn 1973) that enables us to write the determinant of a Hermitian matrix (**FG** in this example), in terms of the two square sub-matrices **A** and **B**

$$\left.\begin{aligned} \mathbf{FG} &= \begin{pmatrix} \mathbf{A} & \mathbf{W}^{T} \\ \mathbf{W} & \mathbf{B} \end{pmatrix}, \\ |\mathbf{FG}| &= |\mathbf{B} - \mathbf{W}\mathbf{A}^{-1}\mathbf{W}^{T}| = |\mathbf{A}||\mathbf{B}||\mathbf{I} - \mathbf{B}^{-1}\mathbf{W}\mathbf{A}^{-1}\mathbf{W}^{T}|. \end{aligned}\right\} \tag{15}$$

If required one can proceed further and factorize the (square) **A** and **B** matrices in a

similar way. This general result will enable us to factorize either the **FG** matrix, or the **F** and **G** matrices separately, in different forms. Once we factorize the matrices we can use local modes for one sub-matrix, **A** for example, and normal modes for the second, the **B** matrix in this example. The use of local against normal modes is dictated by the strength of the coupling in each sub-matrix, i.e. by the ratio between non-diagonal and diagonal terms, and by the approximations that we wish to employ. As the coupling in our problem involves both kinetic (**G** matrix) and potential (**F** matrix) energies the choice of basis set may not always be trivial. However, regardless of the complexity of the solute and/or of the solvent the **F** and **G** matrices can always be written in terms of internal coordinates of the solute degrees of freedom, the solvent–solute relative separation, the pure solvent coordinates and the coupling between these three sub-systems.

3. The reaction rate in the gas phase and in solution

To express the rate constant in terms of a gas phase rate constant times a liquid correction factor we retain the local mode non-diagonal form of the rate constant, equation (13), and use the mathematical result (15). The resulting expression

$$k(T) = k_{\text{gas}} K_{\text{liq}} \tag{16}$$

is interpreted in the following way. k_{gas} is the conventional gas phase rate constant written in terms of local coordinates, i.e. a gas phase barrier crossing frequency, ν^*_{gas}, times a ratio between functions of determinants of tensors of inertia and of the **FG** sub-matrix **S**, defined in (14), times an exponential gas phase Boltzmann factor

$$k_{\text{gas}} = \nu^*_{\text{gas}} \frac{|\mathbf{I}^{\ddagger}_{\text{gas}}|^{1/2}}{|\mathbf{I}^{\text{r}}_{\text{gas}}|^{1/2}} \frac{|\mathbf{S}^{\ddagger}|^{-1/2}}{|\mathbf{S}^{\text{r}}|^{-1/2}} \exp(-\Delta E_{\text{gas}}/k_{\text{B}}T). \tag{17}$$

In equation (17) the superscript as before refers to the TS(‡) or reactants (r), $\mathbf{I}_{\text{gas}}$ is the 3×3 moment of inertia tensor of the isolated solute and **S**, as defined in (14), includes only the solute internal modes. ΔE_{gas} is the difference in energy between the TS and the reactants in the gas phase, i.e. it does not include the possible effect of differences in the solvation of the TS and of the reactants. The liquid phase correction factor of equation (16), K_{liq}, is defined by equations (16) and (17). It is not identical to the, so called, transmission coefficient of TST (Glasstone *et al.* 1944) and need not be bounded by unity. By its very definition it is expressed as a product of ratios between barrier crossing frequencies, geometrical factors, vibrational amplitudes, and an exponential solvation energy factor

$$K_{\text{liq}} = \frac{\nu^*}{\nu^*_{\text{gas}}} \frac{|\mathbf{I}^{\ddagger}|^{1/2}}{|\mathbf{I}^{\ddagger}_{\text{gas}}|^{1/2}} \frac{|\mathbf{I}^{\text{r}}_{\text{gas}}|^{1/2}}{|\mathbf{I}^{\text{r}}|^{1/2}} \frac{|(\mathbf{K} - \mathbf{C}\mathbf{S}^{-1}\mathbf{C}^{\text{T}})^{\ddagger}|^{-1/2}}{|(\mathbf{K} - \mathbf{C}\mathbf{S}^{-1}\mathbf{C}^{\text{T}})^{\text{r}}|^{-1/2}}$$

$$\times \frac{|(\mathbf{B} - \mathbf{W}\mathbf{A}^{-1}\mathbf{W}^{\text{T}})^{\ddagger}|^{-1/2}}{|(\mathbf{B} - \mathbf{W}\mathbf{A}^{-1}\mathbf{W}^{\text{T}})^{\text{r}}|^{-1/2}} \exp(-\Delta\lambda/k_{\text{B}}T). \tag{18}$$

The first term on the right-hand side of equation (18) is the ratio between the barrier crossing frequency in the gas phase to that in the liquid. In the second part of this review we discuss this factor in detail and argue that for a typical activated bimolecular reaction in an inert solvent this ratio is close to unity. The reason for this is the large and repulsive forces at the activation barrier that are often comparable to chemical force constants and are larger by one or two orders of magnitude than the solvent–solute interaction.

Mathematically this results in a liquid phase normal mode of the reaction coordinate that at the saddle is very similar to the one in the gas phase, i.e. it is dominated by the reactants gas phase potential energy surface. The rest of K_{liq} can be considered as a ratio of two equilibrium constants: one for the reactants between the solution and the gas phase, and the other for the transition state. Explicitly, the second and third terms on the r.h.s. of equation (18), to which we often refer as a geometrical factor, are the ratio between the determinants of the moments of inertia tensors in the gas phase and in solution at the TS and for the reactants. To a first approximation we may assume that these ratios are close to unity. Considering the other many approximations that are inherent to TST we do not consider this approximation to be a severe one. The way the fourth and fifth term are written is not unique and below we suggest other forms. Here we render their physical origin. The fourth term is a ratio of the different solvent–solute normal modes of vibration at the transition state and for the reactants, modified by the coupling to the pure solute internal coordinates. Similarly, the fifth term describes a similar ratio between vibrational amplitudes but this time of the pure solvent internal modes that are being modified by the coupling to the solute and to the solvent–solute local modes. Finally the exponential factor, $\Delta\lambda$, accounts for the different solvation energies of the TS and of the reactants. In many reactions it is well known that this exponential factor governs the order of magnitude of the reaction rate.

Written in this form of local internal coordinates that are being successively factorized, the liquid phase TST rate constant has a simple physical interpretation that conforms with the hierarchy of interactions suggested by Adelman (1983). It reflects the gradual effect of the solvent on the solute in the following form: first and foremost there are the solvent–solute internal modes that in principle may be ordered in terms of geometrically successive solvation shells that surround the reactive system (Tarjus and Kivelson 1991). The order of these solvation shells may change in the course of reaction and so may the nature of interactions. Specifically so if the reaction involves an ionic species and/or a change in charge distribution. These solvent–solute modes are coupled to the pure gas phase solute modes via both kinetic and potential terms, **C**. Finally, the solvent–solute internal coordinates, **K**, are succeeded by the pure solvent modes, **B**. These last solvent modes are coupled to each other and to the former two hierarchies, i.e. pure solute and solvent–solute modes.

Pictured in this way the rate constant reflects the route in which energy is being consumed and/or dissipated by the reactive system in solution. In any activated bimolecular reaction that takes place in solution the energy needed to surmount the chemical barrier to reaction is supplied by the solvent degrees of freedom, as the reactants have only a thermal energy distribution. Via both kinetic and potential coupling this energy first travels from the solvent modes to the solvent–solute modes and then finally to the reactive system itself. Using time reversibility one can view the dissipation of energy by the products to the solvent in a similar form. Being an averaged quantity the rate constant does not hold in it any information about the specific way in which the energy is being consumed and/or dissipated. This is a detailed microscopic dynamical information and to attain it we go beyond TST in the second part of this review and discuss the actual dynamics in more detail.

Finally, before making any approximations or change of coordinate system that will enable us to express the rate constant in terms of effective volumes we note that the functions of the determinants of both the solvent–solute internal coordinates and the solvent modes that show up in the expression for K_{liq}, equation (18), can be rewritten in the following form

$$K_{\mathrm{liq}} = \frac{v^*}{v^*_{\mathrm{gas}}} \frac{|\mathbf{I}^{\ddagger}|^{1/2}}{|\mathbf{I}^{\ddagger}_{\mathrm{gas}}|^{1/2}} \frac{|\mathbf{I}^{\mathrm{r}}_{\mathrm{gas}}|^{1/2}}{|\mathbf{I}^{\mathrm{r}}|^{1/2}} \frac{|\mathbf{K}^{\ddagger}|^{-1/2}}{|\mathbf{K}^{\mathrm{r}}|^{-1/2}} \frac{|\mathbf{B}^{\ddagger}|^{-1/2}}{|\mathbf{B}^{\mathrm{r}}|^{-1/2}} \frac{|(\mathbf{I}-\mathbf{K}^{-1}\mathbf{C}\mathbf{S}^{-1}\mathbf{C}^{\mathrm{T}})^{\ddagger}|^{-1/2}}{|(\mathbf{I}-\mathbf{K}^{-1}\mathbf{C}\mathbf{S}^{-1}\mathbf{C}^{\mathrm{T}})^{\mathrm{r}}|^{-1/2}} \times \frac{|(\mathbf{I}-\mathbf{B}^{-1}\mathbf{W}\mathbf{A}^{-1}\mathbf{W}^{\mathrm{T}})^{\ddagger}|^{-1/2}}{|(\mathbf{I}-\mathbf{B}^{-1}\mathbf{W}\mathbf{A}^{-1}\mathbf{W}^{\mathrm{T}})^{\mathrm{r}}|^{-1/2}} \exp(-\Delta\lambda/k_{\mathrm{B}}T). \tag{19}$$

If we use this form and rewrite the expression for the rate constant, equation (17), the above mentioned hierarchy of interactions in the expression for the rate constant is even more explicit

$$k(T) = v^* \frac{|\mathbf{I}^{\ddagger}|^{1/2}}{|\mathbf{I}^{\mathrm{r}}|^{1/2}} \frac{|\mathbf{S}^{\ddagger}|^{-1/2}}{|\mathbf{S}^{\mathrm{r}}|^{-1/2}} \frac{|\mathbf{K}^{\ddagger}|^{-1/2}}{|\mathbf{K}^{\mathrm{r}}|^{-1/2}} \frac{|\mathbf{B}^{\ddagger}|^{-1/2}}{|\mathbf{B}^{\mathrm{r}}|^{-1/2}} \frac{|(\mathbf{I}-\mathbf{K}^{-1}\mathbf{C}\mathbf{S}^{-1}\mathbf{C}^{\mathrm{T}})^{\ddagger}|^{-1/2}}{|(\mathbf{I}-\mathbf{K}^{-1}\mathbf{C}\mathbf{S}^{-1}\mathbf{C}^{\mathrm{T}})^{\mathrm{r}}|^{-1/2}} \times \frac{|(\mathbf{I}-\mathbf{B}^{-1}\mathbf{W}\mathbf{A}^{-1}\mathbf{W}^{\mathrm{T}})^{\ddagger}|^{-1/2}}{|(\mathbf{I}-\mathbf{B}^{-1}\mathbf{W}\mathbf{A}^{-1}\mathbf{W}^{\mathrm{T}})^{\mathrm{r}}|^{-1/2}} \exp(-\Delta\lambda/k_{\mathrm{B}}T). \tag{20}$$

Thus within the limits of the usual approximations used in the derivation of a TST rate constant the rate in solution reflects, in successive order, the bare solute, the solvation shells that surround it, and the interactions between the different solvation shells.

We now examine the different approximations that may be utilized in the analysis of this last equation. We start with the ratio between correction factors and in particular with the last one that accounts for the shift in the solvent normal modes due to the solvent–solute modes and the pure solute modes. At the transition state one may reasonably assume that the numerator is roughly unity for the following reason. In the region of the transition to reaction the interaction between the solute molecules is dominated by the gas phase potential energy surface and it is comparable to chemical forces (Ben-Nun and Levine 1992a, b, Charutz and Levine 1993). Thus the inverse of these frequencies will be a small number and in addition the coupling of the solvent modes to both the solute, and the solvent–solute internal modes will typically be smaller by an order of magnitude or even more. For these two reasons one may in certain cases neglect the last correction term in equation (20). (Approximating the denominator to be one is motivated mainly by the second reason although even for the reactants the attractive interactions will correspond to chemical forces.)

Although we have just reasoned why one can neglect the correction term to the solvent normal modes we may not always wish to do so. In particular we will argue below that the neglect of this term corresponds to a neglect of a large part of the internal pressure that is induced by the cohesive forces that hold the liquid together.

The next viable approximation that one may wish to make is to cancel out the ratio between the unmodified solvent modes, the **B** determinants, at the transition state and for the reactants. Physically this approximation may even be better justified than the previous one as it concerns the unmodified pure solvent–solvent local modes. As one recedes from the solute these modes are likely to be less and less modified when the system evolves along the reaction coordinate. In practice it is obvious that we will consider this approximation only if we have decided upon the former one, i.e., one does not simplify the problem by neglecting the unmodified modes and keeping their correction terms.

3.1. *A geometric free volume and a phase space effective volume*

Regardless if we choose to neglect any term in the expression for the rate constant, or to treat the exact expression, i.e. equation (20), the **S**, **K**, and **B** determinants can always be written in terms of three different uncoupled sets of normal modes. This will enable us to define a generalized effective volume in a phase space that corresponds

to the three different sets of normal modes and thus relate our formalism to cell theory and to the 'classical' geometric free volume. Whereas for the **B** matrix the use of a separate set of normal modes is often the correct procedure, using two disjoint sets for the solute and solvent–solute part is often not very instructive. The reason is the correction term for these two distinct sets that may be large if the magnitude of the non-diagonal terms, **C**, in the original **A** matrix is large with respect to the **S** and **K** terms. Thus depending on the magnitude of the coupling one chooses to work with three (**S**, **K** and **B**), or two (**A** and **B**) disjoint sets of normal modes. Written in terms of sets of normal modes the exact expression for the rate constant is factorized into a product of normal modes times a correction factor

$$k(T) = \nu^* \frac{|\mathbf{I}^{\ddagger}|^{1/2}}{|\mathbf{I}^{\mathrm{r}}|^{1/2}} \frac{\left(\prod_{\text{solute}} \lambda_i^{\ddagger}\right)\left(\prod_{\text{solvent–solute}} \delta_i^{\ddagger}\right)\left(\prod_{\text{solvent}} \chi_i^{\ddagger}\right)}{\left(\prod_{\text{solute}} \lambda_i^{\mathrm{r}}\right)\left(\prod_{\text{solvent–solute}} \delta_i^{\mathrm{r}}\right)\left(\prod_{\text{solvent}} \chi_i^{\mathrm{r}}\right)} \exp(-\Delta E/k_{\mathrm{B}}T)$$
$$\times \frac{|(\mathbf{I} - \mathbf{K}^{-1}\mathbf{C}\mathbf{S}^{-1}\mathbf{C}^{\mathrm{T}})^{\ddagger}|^{-1/2}}{|(\mathbf{I} - \mathbf{K}^{-1}\mathbf{C}\mathbf{S}^{-1}\mathbf{C}^{\mathrm{T}})^{\mathrm{r}}|^{-1/2}} \frac{|(\mathbf{I} - \mathbf{B}^{-1}\mathbf{W}\mathbf{S}\mathbf{A}^{-1}\mathbf{W}^{\mathrm{T}})^{\ddagger}|^{-1/2}}{|(\mathbf{I} - \mathbf{B}^{-1}\mathbf{W}\mathbf{A}^{-1}\mathbf{W}^{\mathrm{T}})^{\mathrm{r}}|^{-1/2}}. \tag{21}$$

In equation (21) the λ_i's are the normal modes of the reactive system calculated as if there is no coupling to the solvent, i.e., the **S** sub-matrix is decoupled from the other matrices, and δ_i and χ_i, are the solvent–solute, and solvent–solvent normal modes, respectively. These normal modes are also calculated as if each subset of coordinates, **K** and **B**, is isolated from the rest of the system. Equation (21) is similar to the form of the TST rate constant of the Caldeira–Leggett Hamiltonian (Caldiera and Legget 1983a, b) and to the Grote–Hynes expression for the rate of reaction derived from a generalized Langevin equation (Grote and Hynes 1980, Hynes 1985a). The Caldeira–Leggett Hamiltonian describes a reactive particle that is linearly coupled to a bath of N distinct harmonic oscillators. This Hamiltonian can be shown to be analogous to the stochastic GLE equation studied by Hynes *et al.* (Adelmann 1983, Chandler 1986, Pollak 1986a, b, 1987, Talkner and Braun 1988, Zwanzig 1987). In both cases the rate is written as a gas phase rate constant times a correction factor that is given by a product of normal modes. Equation (21) has a similar form. We have the bare gas phase normal modes of the solute that are part of the gas phase rate constant times the normal modes of the solvent and of the solvent–solute relative motion (the rest includes a gas phase frequency factor and a moment of inertia tensor, see equation (17)). The solvent–solvent and solvent–solute normal modes are further corrected to account for their mutual presence (and for the presence of the solute itself). As noted by Grote and Hynes (1980), this correction term may be quite large thus indicating that the choice of basis set is not optimal and one should back up and treat the solute and solvent–solute coordinates as a single basis set in the normal mode analysis. This results in two manifolds of normal modes and a single correction term for the solvent modes

$$k(T) = \nu^* \frac{|\mathbf{I}^{\ddagger}|^{1/2}}{|\mathbf{I}^{\mathrm{r}}|^{1/2}} \frac{\left(\prod_{\text{rest}} \eta_i^{\ddagger}\right)\left(\prod_{\text{solvent}} \chi_i^{\ddagger}\right)}{\left(\prod_{\text{rest}} \eta_i^{\mathrm{r}}\right)\left(\prod_{\text{solvent}} \chi_i^{\mathrm{r}}\right)} \exp(-\Delta E/k_{\mathrm{B}}T) \frac{|(\mathbf{I} - \mathbf{B}^{-1}\mathbf{W}\mathbf{S}\mathbf{A}^{-1}\mathbf{W}^{\mathrm{T}})^{\ddagger}|^{-1/2}}{|(\mathbf{I} - \mathbf{B}^{-1}\mathbf{W}\mathbf{S}\mathbf{A}^{-1}\mathbf{W}^{\mathrm{T}})^{\mathrm{r}}|^{-1/2}}. \tag{22}$$

In equation (22) the label 'rest' refers to the solute and solvent–solute internal coordinates, i.e., to the original **A** matrix. The normal modes of the reactive system no

longer correspond to that of the bare gas phase reactive potential energy surface and depending on the strength of the coupling will include more (or less) of the solvent–solute motion in them.

Once we have closed the cycle and went back to normal mode coordinates, we recover the free volume by noting that the different sets of normal modes (i.e., λ, δ and χ of equation (21) or η and χ of equation (22) are just a product of vibrational partition functions with the general form

$$\prod_i \rho_i^j = \prod_i \frac{k_B T}{h\nu_i}, \quad \text{and } \rho^j = \lambda, \delta, \chi \text{ or } \eta, \chi. \tag{23}$$

The amplitude of the normal mode reflects the effective volume in phase space in which each mode is allowed to move. This effective volume is more general than the one given by cell theory. The latter results from an averaged mean-field theory and it is interpreted as a 'true' physical motion of the reactive system in some effective cell that is the result of averaging over both the solvent–solvent and solvent–solute interactions (Hirschfelder 1939). As a result of this averaging the 'cell theory' TST rate constant is written as

$$\begin{aligned} k(T) &= k_{gas}\left(\frac{\vartheta_f^{\ddagger}}{\vartheta_f^{r}} \exp(-\Delta\lambda/k_B T)\right) \\ &= \left(\frac{kT}{h}\frac{Q_{gas}^{\ddagger}}{Q_{gas}^{r}} \exp(-\Delta E_{gas}/k_B T)\right)\left(\frac{\vartheta_f^{\ddagger}}{\vartheta_f^{r}} \exp(-\Delta\lambda/k_B T)\right). \end{aligned} \tag{24}$$

where ϑ_f is the free volume of the TS molecule ($\ddagger$) or of the reactants (r) in solution, Q_{gas} is the gas phase (i.e., vibration, rotation and internal degrees of freedom) partition function of the reactants or the TS, and $\Delta\lambda$ is, as before, the difference in solvation energies between the TS and the reactants. When we compare this expression to our original exact expression for the rate constant, equation (20), we see that what cell theory does is to average over all local coordinates, except those that are explicit to the solute, in such a way that the effect of the solvent–solvent interactions and even more that of the direct interaction between the solute and the solvent is described by a single configurational integral that results in the free volume.

There are two main differences between cell theory, equation (24), and the exact expression that is written in terms of normal modes, equations (21) or (22). Cell theory only considers a single averaged geometrical cell whereas the exact expression compromises three types of cells. Depending on the coupling each of these cells may have more (or less) of the solute, solvent–solute and pure solvent character. In the exact expression use is made of normal modes and thus the space that maintains these cells is not a geometric one, like in cell theory, and in the original geometrical space some of these phase space cells may substantially overlap each other if they are strongly coupled.

Another formulation that would relate us to free volume is based on the use of a valence force approximation (Bjerrum 1914, Wilson *et al.* 1955). In this formulation the forces considered are those that resist the compression or extension of local bonds and those which oppose the bending or torsion of bonds. Forces between atoms that are not directly bonded are neglected and the potential energy surface is written as a sum of quadratic terms in these coordinates. This may greatly simplify the calculation of the configurational integral, as it will be immediately written as a product of

one-dimensional integrals: one integral for each quadratic term in the potential energy. Each of these integrals would result in a single vibrational amplitude that corresponds to the effective volume of that particular valence bond. Unlike cell theory which uses a vector notation and results in a three-dimensional vibrational amplitude, valence bond theory results in one-dimensional amplitudes. Some of these amplitudes will correspond to stretching bonds yet, they would also compromise bending and torsion amplitudes. Furthermore, we note that to actually get a vibrational amplitude from an integral over position one needs to multiply, and thus divide, by the corresponding momentum partition function. Now, the actual computation of the momentum partition functions is done, as before, by using a Cartesian coordinate system and it therefore results in a product of de Broglie wavelengths, equation (7). When all these operations are performed they account for the Jacobian of the transformation from a diagonal Cartesian kinetic energy mass matrix to a generally non-diagonal valence bond kinetic energy mass matrix. Although the use of valence bond theory may greatly simplify the problem it is not clear how in practice one can construct a reasonable valence bond potential for the solvent and solute. One way of reducing the complexity of the problem would be to divide the solvent into two parts. The first part is considered to be an integral part of the reactive system. A valence bond potential is then composed for the reactive system and a few solvent molecules adjacent to it that have a major contribution to the solvation of the reactants or of the TS. The effect of the rest of the solvent molecules is described in an averaged way using a single mean field potential energy term which, in general, would be different at the TS and for the reactants.

3.2. *The Kramers description*

In the molecular picture that we have so far used, the origin of the difference between the reaction rate in the gas phase and in solution is the possibly quite different structure of the TS (and also of the reactants) for the two cases. Unless the coupling of the solvent to the solute is the same at the barrier and for the separated reactants, the two rates will differ and an explicit example is discussed in section 5. The example also brings out the participation of the solvent motion in the crossing of the barrier. It is possible to approach the problem from a Langevin (or, equivalently, a Fokker–Planck) equation point of view (Fleming and Wolynes 1990, Grote and Hynes 1980, Hänggi *et al.* 1990, Kramers 1940) in which case the correction term K_{liq}, equation (18), acquires a seemingly different meaning. In principle, since one can rewrite the exact dynamics in a Langevin form, the correction term can account even for deviation from the assumption of no recrossing which is inherent to TST. In practice, the approximations which are made in the solution of the Langevin equation are often such that all that is really corrected for is the need to redefine the transition state (from what it was in the gas phase) due to the coupling of the solvent to the solute. The resulting correction is then just the K_{liq} term, as discussed earlier. This term can deviate considerably from unity (and in either direction) even if there is no energetic factor due to preferential solvation. It is however a result of the different nature of the TS in the gas phase and in solution (and ditto for the reactants).

There can be deviations from the transition state assumption that it is the rate of the crossing of the activation barrier that is rate determining. The Kramers approach can account for these. An alternative approach, and one that is in the spirit of the gas phase point of view that we use in this review, is discussed in the next subsection.

3.3. *Activation control, diffusion control and cage control*

The net rate of an activated bimolecular reaction in solution is a result of at least two processes: the diffusion of the reactants into a mutual solvating shell and the actual crossing of the activation barrier to reaction. So far, we have assumed that the rate is determined by the activated barrier crossing. Here we discuss a possible modification that interpolates, in a smooth fashion, between the limit of a diffusion controlled reaction and a barrier crossing limiting step, without any assumption about any time separability of the two processes. The new parameter that enters into our considerations is the rate with which the reactants collide once they have approached to within the foothills of the activation barrier and are not separated from one another by one or more solvent molecules. In other words, we will distinguish between the rate with which the reactants approach one another from the bulk and get into the cage (sometimes known as the 'encounter rate' North (1964)) which we denote as k_{diff}, and their collision rate inside the cage, which is physically the analogue of the gas phase collision frequency, and which will be denoted below as Z.

It was suggested by Troe (1986) that the reaction rate in solution can be expressed as

$$\frac{1}{k} = \frac{1}{k_{\text{diff}}} + \frac{1}{k_{\text{react}}}. \tag{25}$$

Here k_{react} is the rate implied by transition state theory for the crossing of the activation barrier. For diffusion limited reactions $k_{\text{diff}} < k_{\text{react}}$ and the opposite is true for direct reactions. Equation (25) is in the spirit of the Lindemann–Hinshelwood mechanism (Weston and Schwartz 1972) for unimolecular reactions. To see the implicit assumption that is involved in deriving (25), it is convenient to rewrite it as

$$k = k_{\text{diff}} \frac{k_{\text{react}}}{k_{\text{react}} + k_{\text{diff}}} = k_{\text{react}} \frac{k_{\text{diff}}}{k_{\text{react}} + k_{\text{diff}}}. \tag{26}$$

This shows that the probability of the reactants getting out of their cage (whether into the bulk or into products), see figure 1, is independent as to how they got into the cage. In other words, the reactants have stayed long enough in the cage to have forgotten the entrance through which they came in. As will be emphasized below, the sojourn in the cage may be for a finite duration so that one must allow for the possibility that this RRK type of assumption will fail.

From the point of view of the supramolecule, the cage is a barrier as shown in figure 1. In a unimolecular reactions of larger molecules, or of ions, one often has more than one barrier and one then sometimes speaks of 'transition state switching', corresponding to which one of the crossings is rate determining (Lifshitz *et al.* 1991).

When one cannot define a 'surface of no return' through which those trajectories which start as the separated reactants and proceed to form products, go only once, we can still use the probability branching analysis of Hirschfelder and Wigner (1939), see also Miller (1976). This analysis expresses the probability of going from a to b as a sum over all possible 'branches'. The different branches correspond to reactants that have survived n oscillations back and forth within the cage. For $n = 1$ the net reaction probability reduces to the TST result whereas in the other extreme limit of $n \gg 1$ the result (25) is recovered. Each branch in the sum corresponds to the following event: the reactants have entered the cage and have survived n oscillations in a joint solvation shell before its exit towards products. Such a probability is the product of the probability of entering a joint solvation shell (this probability is directly related to the solvent barrier

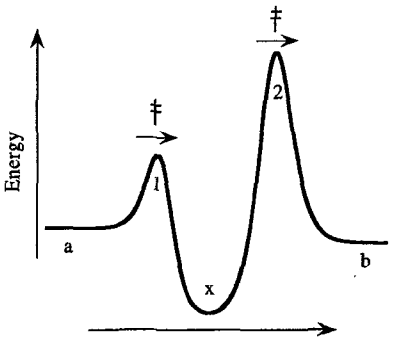

Figure 1. Sketch of a one-dimensional energy profile for an activated reaction in solution. (This plot is the energy along the reaction coordinate for the supramolecule.) The letters a, b, and x designate the *separated* reactants, products and reactants that are confined to a single solvation shell, respectively. Note that in principle, a third barrier may exist en route from products in a mutual solvation shell to the well separated products. The first barrier is that for the separated reactants to cross into a joint solvation shell. There may well be such a barrier even if there is a long-range attraction between the isolated reactants due to a solvent-separated pair. See section 6 for a specific example. The second barrier is the activation barrier to reaction. The height of this barrier will typically depend also on the solvent–solute coupling and so, need not be the same as the barrier height in the gas phase. The parameters that govern the total rate of reaction are the diffusion rate into a mutual solvation shell k_{diff}, the collision rate Z of the reactants at the foothills of the activation barrier, i.e., the rate of crossing of a dividing surface at x, and the actual rate of crossing the barrier to reaction k_{react} as given by TST. For the example shown, the total rate would, to a large extent, be activation controlled.

crossing rate), the probability that the supramolecule survives n oscillations in the mutual solvation shell without recrossing back to the separated reactants or forward to the products, times the probability that the supramolecule does cross the chemical barrier and forms products (this probability is determined by the rate of crossing the chemical barrier to reaction). The resulting expression for the total probability, $P_{b\leftarrow a}$, of going from separated reactants (a) to products (b),

$$P_{b\leftarrow a}=\frac{P_{b\leftarrow x}P_{x\leftarrow a}}{P_{b\leftarrow x}+P_{a\leftarrow x}-P_{b\leftarrow x}P_{a\leftarrow x}} \tag{27}$$

correctly extrapolates between diffusion limited reactions to the ones governed by the chemical barrier to reaction. In equation (27) $P_{x\leftarrow a}$ and $P_{b\leftarrow x}$ are the probabilities of crossing the solvent barrier from solvent separated reactants into the cage and that of crossing the chemical barrier from the cage and into products, respectively. $P_{a\leftarrow x}$ is the finite probability of exiting from the cage into the region of solvent separated reactants. Inspection of this more general result shows that it correctly reduces to the two known limits. For diffusion limited reactions, once the products got into the cage they will, with high probability, react or $P_{b\leftarrow x}\gg P_{a\leftarrow x}$ so that the probability of going from reactants to products is given by the diffusion probability, $P_{b\leftarrow a}=P_{x\leftarrow a}$. The opposite is true when the probability of the caged reactants to go back into separated reactants is small so that the $P_{b\leftarrow a}$ is given by the Troe limit, i.e., equation (25). For intermediate cases, the complete expression has to be evaluated. This requires one further input beyond that required for the limiting form (26). It is convenient to choose that input as the rate, Z, of collisions of the reactants inside the cage. In a TS terminology,

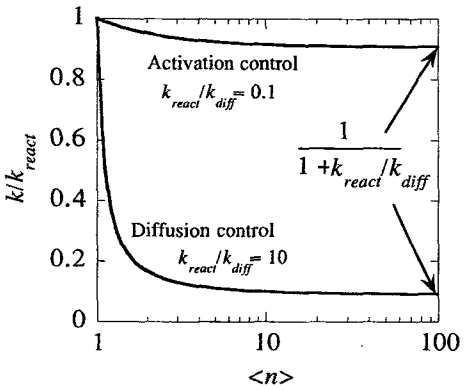

Figure 2. The net rate of an activated reaction measured in units of the rate of crossing the activation barrier to reaction, as given by equation (28) against the mean number $\langle n \rangle$, of crossings of the cage, plotted on a logarithmic scale. The two lines correspond to activation limited (upper line) and diffusion limited (lower line) reactions. The correction to Troe's formula, equation (25), is seen to be important only for $\langle n \rangle < 10$.

this is the rate of crossing of a dividing surface at x. At this configuration the reactants are within the cage so that they are closer in than the solvent separated reactants. On the other hand they are not yet so close as to be within the range of the repulsive barrier potential. The Troe limit, equation (25) or (26), corresponds to many collisions within this case. The distinction that we are making between the rate of diffusion and Z is the same one made in the kinetics literature (North 1964) between the rate of encounters and the rate of collisions in solution. The more general case is derived as follows.

The probabilities $P_{x \leftarrow a}$ and $P_{a \leftarrow x}$ correspond to crossing of the same TS, the first one in figure 1. Their ratio is therefore Z/k_{diff} where Z is the rate of crossing of the dividing surface at x. It follows that the net reaction rate has the form

$$k = k_{\text{react}} \frac{k_{\text{diff}}}{k_{\text{diff}} + k_{\text{react}} - k_{\text{diff}} k_{\text{react}}/Z}. \tag{28}$$

If those reactants that have entered the cage proceed immediately to react, $Z = k_{\text{diff}}$ and $k = k_{\text{react}}$. This is the strict TS limit. On the other hand, if many collisions take place within the cage, $Z > k_{\text{diff}}$ and one recovers the Troe limit, equation (26). In terms of the mean number, $\langle n \rangle$, of crossings of the cage, one finds, see figure 2, that deviations from the Troe limit, requiring the use of equation (28), are important only for $\langle n \rangle < 10$. In section 5.7 we shall bring forth evidence from the dynamical studies that this is the regime which is typical of not very strongly coupled solvents. A special case of the Troe limit is diffusion control, $k_{\text{diff}} < k_{\text{react}}$, when essentially every pair that enters the cage will react so that $k \cong k_{\text{diff}}$. One should however note that k_{diff} as used here is the rate of diffusion of the reactants from the bulk into their mutual cage. As such, it is a diffusion under the long-range force that operates between the reactants. In section 6 we discuss a case (ion–molecule reaction) where this force is quite dominant.

While the language used is quite different from that employed in the Kramers approach, the intent is not dissimilar. One corrects for the fact that the probability to find the reactants at the foothills of the activation barrier is modified due to the solvent barrier at the entrance to the cage. Further discussion can be found, e.g., in Agmon and

Levine (1993) and references therein. The notions of kinetic against thermodynamic control are also discussed there.

3.4. *Conclusions*

It is possible to relate the reaction rate in solution and in the gas phase by assuming that also in solution it is the crossing of the activation barrier to reaction that is rate determining. There are then three differences that contribute. First, the reactive frequency in the gas phase and in solution need not be the same as the solvent can participate in the barrier crossing. Similarly, the other (perpendicular) frequencies of the reactants and of the transition state can also be modified due to the interaction with the solvent.

4. The reaction rate in solution

The TST expression for the reaction rate constant can be examined not only in reference to the corresponding expression in the gas phase but also with respect to the properties of the reactants and of the solvent. We begin with the latter, with special reference to the concept of internal pressure.

4.1. *The effect of pressure*

Solvent effects on the rate of reactions are often discussed by the use of two terms: cohesive forces (or internal pressure) and chemical pressure. The internal pressure results from the forces that bind the liquid molecules together. Furthermore, a dissolved solute molecule that has a more specific interaction with the liquid is subject to an additional pressure that is termed 'chemical pressure', even though the more specific interaction need not be chemical in nature. For non-polar solvents the chemical pressure is not of primary importance and it does not change much upon change of solvent. This is not the case for a polar or ionic solute in a polar liquid. Here, the 'chemical' interactions around the solute cause the neighbouring solvent cavities to contract in a process known as electrostriction. Polar solutes in a non-polar solvent are an intermediate case. Beyond these are the truly more specific interactions.

Even before considering the effect of the solvent itself on the reaction, rate constants were measured at different external pressures and volumes of activation were obtained (Isaacs (1981) and reference therein, Noyes (1961)). In a given solvent both the reactants and the TS have a certain volume. The difference between the volume of the TS ($V^{\ddagger}$) and that of the reactants (V^{r}) is defined as the volume of activation ($\Delta V^{\ddagger}$) that accompanies a reaction, and it can be related to the pressure dependence of the rate constant (Clark and Wayne 1969, Weston and Schwartz 1972)

$$\left(\frac{\partial \ln k(T)}{\partial P}\right)_T = -\frac{\Delta V^{\ddagger}}{k_B T}. \tag{29}$$

The result (29) is simple and enables one to argue in a manner reminiscent of the use of LeChatelier's principle in equilibrium thermodynamics. For our purpose it must however be supplemented by a molecular level interpretation.

We begin with the pioneering work by Hildebrand (1929), Hildebrand and Wood (1933), Hildebrand and Scott (1962) and of Evans and Polanyi (1935, 1937), see also Glasstone *et al.* (1944). We then proceed to suggest a more rigorous result that may be interpreted in terms of the molecular properties of the system, i.e., the Hamiltonian. Superficially it may look as if our formulation refers to a continuous solvent and, as such, does not provide any molecular information. We would however seek to show

that it does, and that it does not differ much from the preceding part of this review that used partition functions for the formulation of the rate constant.

The original derivation of Hildebrand was based on the idea of regular solutions (Hildebrand and Wood 1993). Regular solutions are composed of symmetrical molecules for which the entropy of mixing is the same as for an ideal solution of the same composition. As a result and by correctly neglecting PV work the difference in free energy between a regular solution and an ideal one is equal to the difference in internal energies, $\Delta G = \Delta E$. Hildebrand next showed that by using the pair (or radial) distribution function, $g(R)$, and by considering only the attractive part of the interactions the activity coefficient of a solute molecule A (f_A) in a solvent S is given by

$$\ln f_A = \left(\frac{V_A}{k_B T}\right)\left[\left(\frac{E_{AA}}{V_A}\right)^{1/2} - \left(\frac{E_{SS}}{V_S}\right)^{1/2}\right]^2. \tag{30}$$

V_A (V_S) is the solute (solvent) volume, and E_{AA} (E_{SS}) are the solute–solute (solvent–solvent) interactions. (To get this result Hildebrand has assumed, as we often do, that the solvent–solute interactions are given by the geometrical average over the individual solvent–solvent and solute–solute interactions, i.e., $E_{AS} = (E_{SS}E_{AA})^{1/2}$.) Next, the internal pressure, P^i, that is defined as the change in internal energy of a system during a small isothermal volume change was identified as $P_X^i = E_{XX}/V_X$ where X could be either A or S. Perceived in this way the internal pressure is related to the molecular details of the attractive interactions: the well depth and length parameter, or to the more bulk averaged a coefficient of the van der Waals (vdW) equation of state (Hirschfelder 1939). Using this result the rate for the reaction of molecules A and B in a solvent S can be written as (Glasstone *et al.* 1944)

$$k_B T \ln k(T) = \text{const} + V_A(\delta_A^i - \delta_S^i)^2 + V_B(\delta_B^i - \delta_S^i)^2 - V^{\ddagger}(\delta_{\ddagger}^i - \delta_S^i)^2. \tag{31}$$

The constant refers to the rate of reaction at some standard state and δ_X^i is the square root of the internal pressure ($X = A, B, \ddagger$ or S).

Equation (31) calls for some interpretation before we proceed with the molecular derivation. As a first approximation one can assume that the chemical interactions with the solvent determine the volumes of the reactants and of the transition state, whereas the solvent structure affects the internal pressure. We further note that equation (31) requires the knowledge of the internal pressure of four different 'solvents': the actual solvent S and three other 'hypothetical' solutions of pure A, B, or TS molecules. To infer from this expression on the effect of internal and/or 'chemical' pressure on the rate of reaction one more assumption is necessary. One assumes that any loosening of bonds is accompanied by a lower internal pressure. This leads to the following conclusions: the effect of internal pressure on non-polar reactions is the same as that of external pressure. Thus the rate of reactions that involve a net loosening of bonds at the TS decreases when the solvent internal pressure increases, and the opposite is true for bimolecular reactions (Dack 1974). For polar reactions the changes in volume are the dominant factor and the effect of internal pressure is minor. Hence, in a polar reaction any solvent that produces a more negative volume of activation increases the rate of reaction. For polar reactions that take place in a non-polar solvent, the effect of solvent internal pressure must still be considered.

The derivation of Hildebrand is a step forward. It considers the effect of solvent–solvent interactions as well as those with the solute and it therefore provides us with a tool for predicting relative rates of reactions in different solvents. There is, however, one primary flaw and a second minor theoretical ambiguity with equation (30).

First, one has to remember that it is 'exact' only for regular solutions. Second, the distinction between internal against chemical pressure is somewhat ambiguous and the neglect of the repulsive interactions is not clear. To better understand and clearly distinguish between internal cohesive forces against chemical electrostriction we appeal to the 'hard' and 'soft' part of the dissolution processes. No approximation is made about the nature of the solution and as a side benefit the rate constant is again written in terms of the molecular Hamiltonian.

We consider the process of dissolution to be composed of two sequential processes: first a cavity is formed at a fixed position and then the interactions with the liquid are switched on and the fixed position restriction is removed (Eley 1939, 1944, Körosoy 1937, Uhlig 1937). The energy associated with the forming of the cavity itself is positive, one needs to invest energy to push away the solvent molecules. The amount of energy required to form the cavity depends on the forces between the liquid atoms and on the size of the cavity which is directly related to the size of the solute molecule. The second part of the dissolution process, the introduction of interactions lowers the energy. If these two processes require energies of similar magnitude the resulting enthalpy, and therefore free energy because ΔPV can be neglected, will have a small positive or negative value. An exceptional case is water. Here hardly any energy is required to build up the cavity, as there are 'natural' cavities in the open structure of water. This results in a large negative value of the standard enthalpy of solvation of inert gases in water. Thus, by separating the solvation processes into two parts the anomalous properties of water are revealed in the first step of forming the cavity.

We now turn to a more detailed quantitative description of the dissolution process (Ben-Naim 1974). Let us assume that the solute–solvent pair potential $U(\mathbf{R}_S, \mathbf{X})$ can be split into two parts, a repulsive hard-core part $U^H(R)$ that depends on the distance between the centres of the solute and the solvent $R = |\mathbf{R}_S - \mathbf{X}|$ and an attractive 'soft' part $U^S(\mathbf{R}_S, \mathbf{X})$ that depends on the location of the solute $\mathbf{R}_S$ and on the location and orientation of the solvent molecule $\mathbf{X}$

$$U(\mathbf{R}_S, \mathbf{X}) = U^H(R) + U^S(\mathbf{R}_S, \mathbf{X}). \tag{32}$$

For this definition to be valid some hard-core diameter σ_H must be associated with the solvent–solute interaction so that

$$U^H(R) = \begin{cases} \infty, & R \leqslant \sigma_H, \\ 0, & R > \sigma_H, \end{cases} \tag{33}$$

and we have further assumed that it does not depend on the relative orientation of the potential. (Note that the letter S has a double meaning: as a subscript it refers to the solute and as a superscript it stands for soft.) The 'soft' part of the potential is defined by the difference between the total potential and the hard-core potential and as such it includes the potential energy dependence on the orientation of the solvent molecules. The hard-core diameter is an effective distance of closest approach that can be estimated as the average of the solvent and solute hard-core diameters. This results in a soft potential that is attractive for most of the solvent–solute configurations. We now introduce two coupling parameters that define an auxiliary potential energy function

$$U(\zeta_1, \zeta_2) = U_M(\mathbf{X}_1 \ldots \mathbf{X}_N) + \zeta_1 \sum_{i=1}^{N} U^H(\mathbf{R}_S, \mathbf{X}_i) + \zeta_2 \sum_{i=1}^{N} U^S(\mathbf{R}_S, \mathbf{X}_i). \tag{34}$$

The first term of the r.h.s. of equation (34) denotes the potential energy associated with the configuration of the solvent molecules and the last two parts involve the idea of a coupling parameter that changes continuously from zero to one. An uncoupled solute

corresponds to the state $\zeta_1 = \zeta_2 = 0$ and a fully coupled solute particle corresponds to $\zeta_1 = \zeta_2 = 1$. This double coupling process is somewhat more involved than the usual coupling of a cavity to the surrounding solvent. We first couple the 'hard' part of the potential to the solvent and then proceed and build up the attractive interactions. Using equation (34) an auxiliary configurational partition function that depends on both coupling parameters is defined and the work of introducing a solute particle into solution is written as a sum of three terms

$$\mu = \bar{\mu}^H + \bar{\mu}^S = k_B T \ln(\rho_S \Lambda_S^3 q_S^{-1}). \tag{35}$$

The first term on the r.h.s. of equation (35) defines the work associated with creating a cavity at a fixed position in the solvent (the size of the cavity is determined by the hard-core diameter which we chose in equation (33)). The second term corresponds to the work gained by turning on the soft part of the interaction potential and finally the last term accounts for the release of the fixed position constraint that we imposed on the cavity and for the internal degrees of freedom of the solute. Λ_S^3 is the three-dimensional de Broglie wavelength of the solute particle, q_S is the partition function of the rotational and internal degrees of freedom of the solute particle and ρ_S is an inverse of a volume element which for a single solute particle equals V^{-1}. The integrated Hellman–Feyman theorem provides an explicit form of the 'hard' $\bar{\mu}^H$ and 'soft' $\bar{\mu}^S$-chemical potentials. It involves a singlet conditional distribution function for a solvent molecule given a fixed solute particle at $\mathbf{R}_S$ coupled to the solvent to the extent of a variable ζ_1 at $\zeta_2 = 0$

$$\left.\begin{aligned} \bar{\mu}^H &= \int_0^1 \mathrm{d}\zeta_1 \int \mathrm{d}\mathbf{X}\, U^H(\mathbf{R}_S, \mathbf{X}) \rho(\mathbf{X}/\mathbf{R}_S, \zeta_1, \zeta_2 = 0), \\ \text{or for a variable } \zeta_2 \text{ at } \zeta_1 = 1 & \\ \bar{\mu}^S &= \int_0^1 \mathrm{d}\zeta_2 \int \mathrm{d}\mathbf{X}\, U^S(\mathbf{R}_S, \mathbf{X}) \rho(\mathbf{X}/\mathbf{R}_S, \zeta_1 = 1, \zeta_2). \end{aligned}\right\} \tag{36}$$

The singlet conditional probability functions are defined by the corresponding potentials and probability functions

$$\left.\begin{aligned} \rho(\mathbf{X}/\mathbf{R}_S, \zeta_1, \zeta_2 = 0) &= N \int \ldots \int \mathrm{d}\mathbf{X}^{N-1} P(\mathbf{X}^N/\mathbf{R}_S, \zeta_1, \xi_2 = 0) \\ &= N \frac{\int \ldots \int \mathrm{d}\mathbf{X}^{N-1} \exp\left\{ -\left[U_N(\mathbf{X}_1 \ldots \mathbf{X}_N) + \zeta_1 \sum_{i=1}^{N} U^H(\mathbf{R}_S, \mathbf{X}_i) \right] \Big/ k_B T \right\}}{Z(\zeta_1, \zeta_2 = 0)}, \\ \text{and} & \\ \rho(\mathbf{X}/\mathbf{R}_S, \zeta_1 = 1, \zeta_2) &= N \int \ldots \int \mathrm{d}\mathbf{X}^{N-1} P(\mathbf{X}^N/\mathbf{R}_S, \zeta_1 = 1, \xi_2) \\ &= N \frac{\int \ldots \int \mathrm{d}\mathbf{X}^{N-1} \exp\left\{ -\left[U_N(\mathbf{X}_1 \ldots \mathbf{X}_N) + U^H(\mathbf{R}_S, \mathbf{X}^N) + \zeta_2 \sum_{i=1}^{N} U^S(\mathbf{R}_S, \mathbf{X}_i) \right] \Big/ k_B T \right\}}{Z(\zeta_1 = 1, \zeta_2)}, \end{aligned}\right\} \tag{3}$$

where the auxiliary configurational partition function is

$$Z(\zeta_1, \zeta_2) = \int \ldots \int \mathrm{d}\mathbf{X}^N \exp[-U(\zeta_1, \zeta_2)/k_B T]. \tag{38}$$

Equation (35) with its complementary definitions, equations (36)–(38), provides a molecular interpretation of the solvation process and its dependence on the coupling process. First, we increase the hard-core interaction ζ_1 from zero to unity, keeping the soft part switched off. Once ζ_1 has attained its final maximal value of unity the process of forming the cavity is complete and ζ_2 is gradually increased from zero to unity. It is important to note that this dissolution process is carried out for the full chemical potential but for the pseudo-chemical potential, denoted by a bar. $\bar{\mu}^H$ is the work needed to form a cavity with a diameter σ_H at a fixed position. It is thus equivalent to the process of introducing a hard-sphere particle with a diameter σ_H at a fixed position. When the fixed position constraint is removed these two processes are no longer equivalent.

Once the chemical potential is written in a split form, equation (35), other thermodynamical properties and in particular the rate constant can be derived. If for example the reactants are composed of molecules A and B the TS rate constant

$$k(T) = \frac{(q_\ddagger \rho_\ddagger^{-1} \Lambda_\ddagger^{-3})}{(q_A \rho_A^{-1} \Lambda_A^{-3} q_B \rho_B^{-1} \Lambda_B^{-3})} \exp\left[-(\Delta\bar{\mu}^H + \Delta\bar{\mu}^S)/k_B T\right] \tag{39}$$

has a simple interpretation. The pre-exponential factor describes the motion of the TS and reactants (A and B in this specific example) cavities, and their rotational and internal degrees of freedom. The exponential energy factor divides the energy difference between the solvated TS and the solvated reactants into two terms. The first is the difference in energies that are needed for the formation of a cavity for the TS molecule and for the reactants. (In this example two distinct cavities are formed for the reactants.) The second is the difference in energies due to different soft solvent–solute interactions at the TS and in the reactants regions. The energy associated with the first hard part of the dissolution process is solely determined by the solvent structure and by the sizes of the solvent and of the solute (the hard-core diameter is taken to be the average value, or some more complicated function, of the solute and solvent effect hard-core diameters) and as such it corresponds to the internal pressure. The chemical pressure is described by the second part of the dissolution process in which the solvent–solute interactions are switched on. Hence, the use of hard and soft parts in the dissolution process enables us to discern the effects of internal and chemical pressures on the rate of reaction and to directly relate them to the molecular properties of the Hamiltonian. Other things being equal, any reaction that involves an increase in the size of the solute en route to the TS, such as the one that occurs in a unimolecular decomposition, would favour a low pressure solvent and vice versa for the opposite case. When the interactions with the solvent are dominant the difference in hard-core energies between the TS and the reactants are relegated compared to the energy gained by turning on the chemical interactions with the solvent. Any solvent that would favour the interactions with the TS would increase the reaction rate. In section 3.4. similar results were discussed using the local properties of the TS and of the reactants. Here these local properties are cast in a different manner. We first consider the energy required to form an ideal effective solvent–solute cell that is solely determined by the solvent internal properties and by the size of the solute (the latter can be either a TS or a reactant molecule). We then consider the energy gained by the possible collapse of this cell due to the soft interactions with the surrounding solvent molecules.

4.2. *Steric factor in solution*

Most textbooks that discuss the steric factor in transition state theory usually express it in terms of ratios of partition functions. The origin of the steric factor is then quite clear and it is attributed to the free rotations of the reactants that are being converted to vibrations at the TS (Benson 1960). Textbooks sometimes argue that at low temperatures the vibrational partition functions are about unity whereas rotational partition functions are assumed to be between 10 to 100. These arguments have been shown to be rather poor as they result in a wrong temperature dependence of the exponential pre-factor of the reaction rate (Johnston 1966, Levine 1990). The origin of this fault is the assumption for the value of the new vibrational partition functions at the transition state. Although it is true that most vibrational partition functions can be approximated to equal unity at the TS this is no longer true as the new vibrations of the TS correspond to very soft bends or internal rotations. As has been demonstrated by Johnston (1966), an analysis of the pre-exponential factor using local bond properties is more revealing. Here we discuss the origin of the pre-exponential factor in solution using similar arguments.

The configuration partition function was written in equation (11) as a geometrical parameter, J, times a function of the temperature times the determinant of the force constant matrix. As mentioned before, the geometrical factor can be written as a product of factors, one for each atom (Herschbach *et al.* 1959)

$$J = \prod_{\alpha=1}^{N} j_\alpha. \tag{40}$$

Using the result that the force constant determinant can always be expressed as

$$|\mathbf{F}| = \omega^2 \prod_{s=1}^{3N-6} F_{ss}, \tag{41}$$

where ω^2 is a numerical constant, negative for unstable complexes such as the TS, the classical rate constant in solution may be written in a form that puts more emphasis on local properties

$$k(T) = \frac{\nu^*}{\omega} \frac{\left(\prod_{\alpha=1}^{N} j_\alpha \prod_{s=1}^{3N-6} l_s\right)^{\ddagger}}{\left(\prod_{\alpha=1}^{N} j_\alpha \prod_{s=1}^{3N-6} l_s\right)^{\mathrm{r}}} \exp(-\Delta E/k_\mathrm{B}T). \tag{42}$$

In equation (42) l_s is the one-dimensional Boltzmann average of the vibrational amplitude calculated for each diagonal term in the potential energy

$$l_s = \int_{-\infty}^{+\infty} \exp(-F_{ss}x^2/2k_\mathrm{B}T)\,\mathrm{d}x = (2\pi k_\mathrm{B}T/F_{ss})^{1/2}. \tag{43}$$

For simple reactions that involve three to four atoms the effort required for calculating the rate constant using local properties or partition functions is about the same. But, for very complex reactions in liquids the use of local properties is vastly simpler. Put in terms of local properties that do not extend over all the collision complex many non-essential terms in the denominator and numerator of equation (42) can be assumed to cancel almost identically. These terms correspond to local bonds and angles that are further away from the reactive site (in a liquid this would actually be the majority of the bonds and angles) so that they are hardly affected by the local changes around the

reactive site. By virtue of these cancellations and by recognizing that at the TS new bonds may be formed, the rate constant is written in a simpler form

$$k(T) = \frac{\nu^*}{\omega} \prod_{\substack{\text{that do} \\ \text{change}}} \frac{(jl)^{\ddagger}}{(jl)^{r}} \prod_{\text{new}} (jl)^{\ddagger} \exp(-\Delta E/k_B T). \tag{44}$$

Other things being equal, the effect of forming new bonds at the TS, or of the softening of certain vibrations that are being converted into bending and/or internal rotations of the TS is easily accounted for. For example, any reaction in a polar solvent that involves a delocalization of charge en route to the TS alters the rate constant in two non-consistent ways. First and foremost the solvation of the TS would be less favourable than that of the reactants, and second the vibrational amplitude or effective volume would increase. Reactions that involve the formation of hydrogen bonds with the solvent at the TS would also affect the rate constant in two opposite ways: the entropy of the TS would be reduced but so will its internal energy, the net effect is likely to be an increase in the rate constant. The double effect of catalysis is easily accounted for by equation (44). Apart from being able to reduce the activation energy for reaction by binding to the reactants the catalyst reduces the initial free translational volume of the reactants. As a result the ratio of products of Jacobian factors, at the TS and for the reactants is increased by a large amount. For bimolecular reactions this effect may be quite marked. The effect of the liquid on atom transfer reactions that do not involve any change in charge distribution can be explained in a similar way. An increase in the rate by an order of magnitude when going from the gas phase to solution is attributed to the loss of the free translational volume, V, of one of the reactants due to the presence of the liquid. In the gas phase the small value of the pre-exponential factor is explained by the reduction of this free translational volume of the reactants to a smaller volume, $R^{\ddagger 2} l^{\ddagger}$, of the collision complex. ($R^{\ddagger}$ and $l^{\ddagger}$ are the distance and vibrational amplitude of the new bond that is being formed at the TS.) In solution this is no longer true, as the translational volume of the reactants is no longer V.

5. Beyond TST: Unfolding the dynamical history of the system

Going beyond transition state theory and elucidating the role of the solvent as the system evolves en route from reactant to products is the subject of the second part of this review. We shall use a Hamiltonian point of view so as to make contact with earlier studies of dynamics in the gas phase. In principle, the Hamiltonian equations of motion for the entire supramolecule can always be reduced to fewer Langevin-like equations of motion for a subset of coordinates. Such a reduction is particularly useful if one can replace the exact frictional terms in such an equation by a practical simple form. As we shall repeatedly emphasize, the time regime of interest to us is very short, shorter than one might have originally thought. It is indeed only quite recently that experimental spectroscopic probing of solvation and of dynamics of dissociation have verified that there is this very short time-scale over which the motion is essentially inertial (Lu *et al.* 1993, McManis *et al.* 1991, Neria and Nitzan 1992, 1994). One can develop approximations for a Langevin like description which are valid in this short time-scale and we will indeed sketch how this can be done. However, we consider that a Hamiltonian point of view is equally, if not more so, useful on the short time-scale of interest.

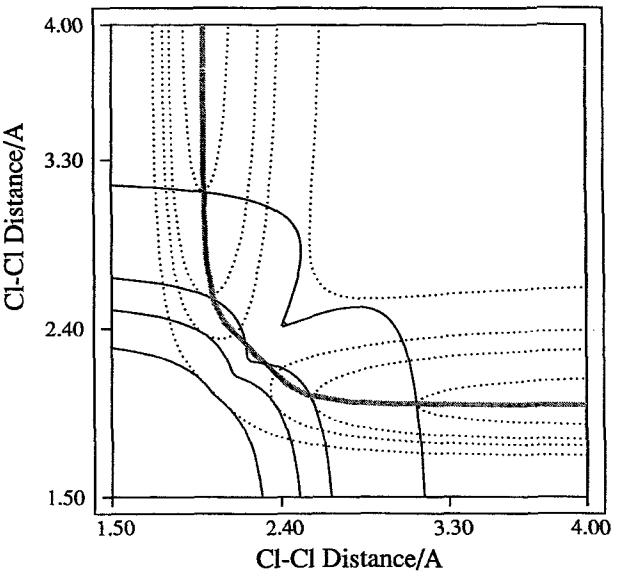

Figure 3. Contour plot of the gas phase interaction potential, V_2, (full line) for the collinear $Cl + Cl_2$ exchange reaction. The potential energy surface (dashed lines) V is of the LEPS functional form with a barrier height of 20 Kcal mol^{-1}. The interaction potential is the part of the gas phase Hamiltonian that vanishes when the reactants (or products) are well separated, e.g., $V_2 = V - V_{diatom}$. The reaction coordinate q is shown as a thick line. The two sets of contours are drawn for the same values of the potential energy in order to emphasize the very localized nature of V_2.

5.1. *The reaction coordinate*

As in the gas phase, it is convenient to begin by examining the energy profile along the reaction coordinate q. Consider first the interaction energy for a typical symmetric $A + BA$ atom exchange reaction as shown in figure 3. The potential along the reaction coordinate is also shown in the upper panel of figure 4. There are two general features characteristic for exchange reactions that we wish to note. One is the relatively short range of interaction: there is a range L, where L is typically of the order of 1 Å, such that at $q = \pm L$ one is already at the very foothills of the barrier. Thus the gas phase interaction region is rather localized. The second important feature is the curvature of the potential. We use the curvature, denoted as $K(q)$ and computed as the second derivative of the potential along q, as a measure for the frequency of the motion. If the motion is bound then its local harmonic frequency is $\omega^2(q) = [K(q)/\mu]$ where μ is the mass. However, even if the motion is unbound, $[-K(q)/\mu]^{1/2}$ locally determines the time-scale of the motion. (Of course, in this case the motion is an unstable one.) Hence the magnitude of the curvature of the potential (scaled by the appropriate mass factor) defines the local time-scale of the motion. At the top of the barrier the magnitude of the unbound force constant is similar to that of a bound diatomic molecule, figure 4 lower panel. Thus the crossing of the barrier is a rapid event, with a typical duration of 10–50 fs. The chemical interactions that operate in the TS region are often stronger by an order of magnitude (or even more) than a typical solvent–solute interaction. If we use the inverse of the local frequency as a measure for the time-scales of the motion, a separation of time-scale is implied by this simple qualitative observation.

The separation of time-scales between the motion along the reaction coordinate

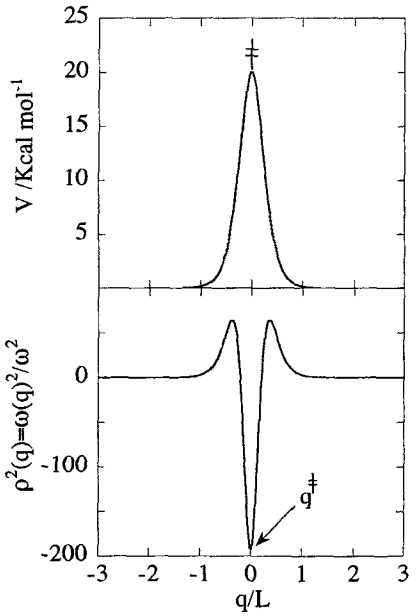

Figure 4. Upper panel: the general features of an energy profile along a reaction coordinate for a symmetric atom exchange reaction against the reaction coordinate q. (L is the range of the potential. Parameters, in both panels, are for the $Cl + Cl_2$ reaction, see figure 3.) The gas phase interaction potential has a short range so that at $q = \pm L$ and $L \approx 2$ Å one is already at the distant foothills of the barrier to reaction, see figure 3. Lower panel: the dimensionless local ratio of the reaction coordinate frequency and the solvent–solute frequency ω, $\rho^2(q) = \omega^2(q)/\omega^2$, along the reaction coordinate, q. The position of the barrier is indicated. The magnitude of the curvature serves as a measure for the local time-scale of the motion. It is the high value of the curvature at the barrier and the low value of ω in rare gas solvents that results in the solvent inability to interfere with the rapid barrier crossing event.

(in the barrier region) and the solvent–solute (and solvent–solvent) relative motions suggests that a small number of solvent–solute modes would suffice for the description of short time-scales dynamics. The model Hamiltonian that we discuss below uses a single effective solvent–solute mode to model the results of the full molecular dynamics simulations. This effective mode is derived from the complete many-body Hamiltonian in the next section.

5.2. *Reducing the dimensionality*

In section 2.1. we discussed the use of local coordinates for computing the reaction rate in solution. These local coordinates are the starting point in our reduction process. Given the many-body Hamiltonian of the supramolecule, we first approximate it using the potential along the reaction coordinate to describe the solute, and express all other couplings by their local values for a given q. These include all other coordinates of the solute (in a manner made familiar by the reaction path Hamiltonian approach in the gas phase (Basilevsky and Rybov 1982, Fischer and Ratner 1972, Hofacker 1963, Hofacker and Levine 1971, Marcus 1966, Miller 1983)), and, in addition, include the solvent–solute and solvent–solvent modes. This may result in a complicated kinetic energy mass matrix **G** (see Hofacker 1963, Marcus 1966) but in general it is always

feasible. Next we expand the liquid potential and the solvent–solute interaction in a Taylor series about some minimum configuration point. (The potential along the reaction coordinate is unaffected by this process.) The resulting force constants matrix **F** has three kinds of coupling: internal to the solute, solvent–solute and solvent–solvent. A normal mode analysis is then performed only on the solvent–solvent modes. The outcome of all these transformations is the following: the potential along the reaction coordinate is unaltered, it is coupled to all the solvent normal modes via potential (and possibly also kinetic) coupling and the latter are diagonal. The result is a reaction path Hamiltonian for the supramolecule. A special case of this Hamiltonian, when we neglect all modes of the solute except for the reaction coordinate q, is sometimes referred to as the Caldeira–Leggett (1983a, b) Hamiltonian and it has often been invoked in the calculation of the TST rate constant in solution. It describes a single reactive solute coordinate (i.e. q) that is bilinearly coupled to N harmonic oscillators that correspond to the liquid bath modes. This mechanical Hamiltonian can be easily recast as a Langevin equation (or GLE for the case of a friction term with memory of the previous history of the system) for the motion along q. The Caldeira–Leggett Hamiltonian assumes that the N normal modes of the bath are stable. This may not necessarily be true in our case and thus we do not exclude the possibility of unstable bath modes that are coupled to the reactive system (Stillinger and Weber 1984a, b). Using matrix notation the **F** matrix that describes the Caldeira–Leggett Hamiltonian has the general form

$$\mathbf{F} = \begin{pmatrix} K(q) & \lambda_1^{\mathrm{T}} & \dots & \lambda_N^{\mathrm{T}} \\ \lambda_1 & k_{11} & & \\ \vdots & & \ddots & \\ \lambda_N & & & k_{NN} \end{pmatrix}. \tag{45}$$

K(q) is the local force constant along the reaction coordinate, λ_i is the coupling strength of the ith solvent normal mode, and k_{ii} is the force constant of the ith mode of the solvent. As noted above, some of these force constants that correspond to unstable modes of the solvent would be negative. Any kinetic solvent coupling can be recast as potential coupling and included in the λ_i's so that the mass matrix **G** is diagonal, but in general **G** would have a non diagonal structure and all the transformations which we next describe would operate on the **FG** matrix.

The inherent separation of time-scales, that is characteristic for activated processes in weakly coupled solvents, allows the use of a single effective solvent–solute mode to mimic the effect of the solvent on the reactive solute at short times. If we rotate the coordinate system using an hermitian matrix **U** we can rewrite equation (45) so that the solute is coupled to a single solvent–solute coordinate and the solvent modes are no longer uncoupled

$$\mathbf{UFU}^{\mathrm{T}} = \begin{pmatrix} K(q) & C^{\mathrm{T}} & \mathbf{0} \\ C & k & \mathbf{y}^{\mathrm{T}} \\ \mathbf{0} & \mathbf{y} & \mathbf{x} \end{pmatrix}. \tag{46}$$

The square matrix **x**, the vector **y**, and the number C are functions of the original solvent normal modes and of the solvent–solute coupling parameters λ_i, equation (45).

The explicit form of the effective solvent–solute force constant k is given by

$$k = \sum_i \lambda_i^2 k_{ii} \Big/ \sum_i \lambda_i^2. \tag{47}$$

This is in the form of a weighted average, with summation over all the normal modes of the solvent. This summation may include a number of unstable solvent modes, but as this number is typically small (and it is weighted by the coupling) the value of k is positive. The form of the effective force constant exhibits the role of both the magnitude of the solvent frequencies and of the spread of these magnitudes. The modes that contribute the most to the value of k have simultaneously a higher frequency and a stronger coupling. This implies that high-frequency modes of a molecular solvent that could be traced back to an internal vibration of the solvent molecule may be neglected, as a first approximation, as their coupling to the solute is likely to be small (Tucker 1993).

Whether the solvent mode that couples to the solute is local against normal in character depends on the nature of the normal modes of the solvent and on the coupling. Even if the normal modes are localized, as would be the case in a monoatomic solvent for example, if a few of them contribute to k, the effective mode would be delocalized over the whole of the solvent. The extent of delocalization would depend on the spread in frequencies (and their corresponding coupling) that have a major contribution to k. As the frequency spectrum of monoatomic liquids is rather narrow (Seeley and Keyes 1989, Wan and Stratt 1994), the effective solvent–solute force constant is expected to be more localized. The mass of the solvent–solute coordinate is given by a similar weighted average and using the same notation the strength of the solvent–solute coupling, C, is given by

$$C^2 = \sum_i \lambda_i^2. \tag{48}$$

Unlike the effective mass or force constant, the value, C, of the coupling increases with the number of solvent modes to which the solute is coupled.

Before proceeding to describe the results of the molecular dynamics (MD) simulations and analysing them using a reduced Hamiltonian we note that if we perform a series of such rotation transformations the resulting force constants matrix would be written in a tridiagonal form

$$\begin{pmatrix} E(q) & C^{\mathrm{T}} & & & & \\ C & k_{11} & k_{12}^{\mathrm{T}} & & & \\ & k_{12} & k_{22} & k_{23}^{\mathrm{T}} & & \\ & & k_{23} & k_{33} & \ddots & \\ & & & \ddots & \ddots & k_{N-1,N}^{\mathrm{T}} \\ & & & & k_{N-1,N} & k_{NN} \end{pmatrix}, \tag{49}$$

and it would describe a sequential hierarchy of interactions in which each mode is directly coupled only to its nearest neighbours via the coupling terms $k_{j,j-1}$ and $k_{j,j+1}$ and only indirectly coupled to all the other modes. The solute is coupled to a solvent–solute mode which is next coupled to a solvent mode etc. This hierarchy of interactions agrees with our physical intuition which views the system as a solute particle coupled to its first solvation shell which is then coupled to a second shell etc.

(Adelman 1983, 1987, Tarjus and Kivelson 1991). In section 3.2. we derived an expression for the TST rate constant that had a similar form, equation (21). The rate in solution was shown to reflect the bare solute, its interaction with the solvent shells that surround it and the interactions between the different solvent shells. The tridiagonal form of the Hamiltonian systematizes these interactions so that a single shell interacts with the solute, and single shells of the solvent interact only with their nearest (upper and lower) shells. One has to remember that these shells do not necessarily correspond to actual successive geometric shells, yet the experimental evidence that the dominant part in the solvation process can be attributed to the first solvation shell (even for an ionic solute) does support this analogy.

5.3. *Molecular dynamics simulations of activated processes*

One of the first striking and intriguing phenomena observed in molecular dynamics simulations of bimolecular atom exchange reactions in rare gas solvents was the absence of the solvent cage effect (Benjamin *et al.* 1990a, b, Bergsma *et al.* 1986, Li and Wilson 1990). By cage effect (Frank and Rabinowitch 1934, North 1964, Schroeder and Troe 1987) we refer to repeated collisions with the solvent first solvation shell that lead to recrossings of the barrier and thus to a decrease in the value of the rate constant. The high value of the curvature $K(q)$ of the potential along the reaction coordinate, figure 4, will be used below to explain the absence of a cage effect in the molecular dynamics simulations of atom–diatom exchange reactions in rare gas solvents. We have shown (Ben-Nun and Levine 1992a) that only at very high densities a clear-cut cage effect is seen, and that even the details of the gas phase potential are important and many trajectories fail to recross the barrier if the isolated gas phase steric and kinematic requirements are not satisfied (Benjamin *et al.* 1990b, Ben-Nun and Levine 1992a), figure 5. The onset of caging is found to be abrupt and it takes place at the same density that self-caging of the solvent becomes important, figure 6. These are also the densities at which, on a longer time-scale, the liquid will seen to be glass-like. (However, at the short times of interest to us one cannot distinguish the phase of the solvent as such distinctions as gas against liquid against glass are only meaningful at times over which diffusion or the absence thereof can be probed.) Rare gas glasses, or rare gas clusters (Liu *et al.* 1993), may therefore provide a useful insight into the dynamical role of the solvent in atom exchange reactions.

The simulations have further shown that the liquid is able to detain the reactants (and/or products) at the distant foothills of the barrier for long periods and that the activation process (or deactivation when looking at the descending products) is localized both in time and in position (Wilson and Levine 1988b). An initial fluctuation that involves a few solvent atoms, adjacent to the reactants, provides the necessary energy to surmount the barrier via a very few hard collisions (Benjamin *et al.* 1990a, b). The activation process takes place a few hundreds of femtoseconds prior to the barrier crossing event and it involves the creation of a hot spot in the liquid (Benjamin *et al.* 1990a, Wilson and Levine 1988).

One should carefully note that we are talking about that subset of trajectories that do manage to scale the barrier. For a system initially in thermal equilibrium there is a far larger subset of non-reactive trajectories. To show that we can discuss only the subset of reactive trajectories it is a convenient to appeal to microscopic reversibility. In the present context this implies that any forward motion in time, that is possible, has an equally possible motion determined by propagating Hamilton's equations of motion backward in time. Any trajectory that ascends to the barrier has as its counterpart a

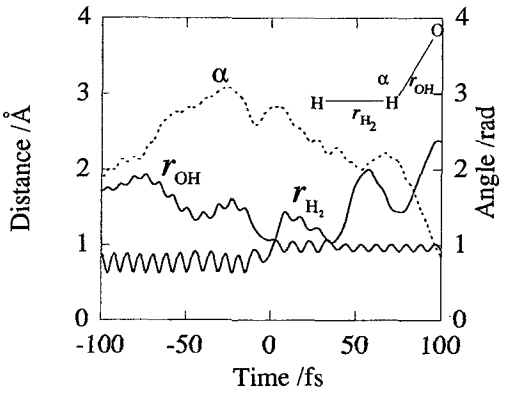

Figure 5. Caging in a dense solvent. Shown are the 'old' and 'new' bond distances against time, computed for the $O + H_2 \rightarrow OH + H$ reaction. The reactants are surrounded by 125 Ar atoms, (the solute–solvent and solvent–solvent interactions are modelled using a pairwise Lennard-Jones (12, 6) potential with a range parameter σ), at a very high reduced density, $\rho^* = \rho\sigma^3 = 1{\cdot}68$. (At a longer time-scale the liquid will become glass like at this density, see figure 6.) Caging is evident as the reactants fail to move apart to such distances that a solvent atom can separate them. Also shown, as a dashed line, the O–H–H angle α. Despite the repeated close approaches, the reactants fail to cross the barrier when the angle α is not near 180°. Examination of the gas phase LEPS potential energy function (Johnson and Winter 1977) shows that the cone of acceptance for the reaction (Levine and Bernstein 1987) is quite narrow. When the bond–bond angle is 150°, the barrier height for reaction exceeds its value for a collinear approach by over 1 Kcal mol^{-1}. Consistent with the earlier work of Benjamin *et al.* (1990), it is the cone of acceptance for the bare gas phase potential that often determines the steric requirements in solution.

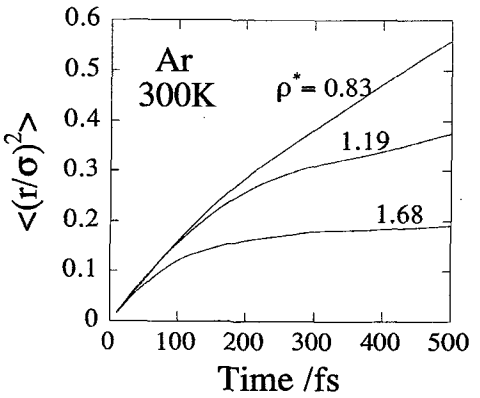

Figure 6. Variance of the distribution of Ar–Ar interatomic distances (in units of σ^2, where σ is the range parameter of the LJ potential, $\sigma = 3{\cdot}4$ Å) against time for three reduced densities at 300 K. Most simulations are carried out at the critical density $\rho^* = \rho\sigma^3 = 0{\cdot}83$ when no caging is evident. On the time-scale of interest, i.e., the barrier crossing time which is less than 100 fs see figure 5, the behaviour of the solvent at $\rho^* = 1{\cdot}68$ is not qualitatively different from that at $\rho^* = 0{\cdot}83$. If the time axis is scaled by an order of magnitude, so that it runs to 5 ps, then the behaviour at $\rho^* = 0{\cdot}83$ will be seen to be diffusive ($\langle r^2 \rangle \propto t$), whereas at $\rho^* = 1{\cdot}68$ the rare gas atoms themselves become caged and the solvent is glass-like.

trajectory that descends from the barrier. This is a result that we will appeal to below. It also offers a rationalization of why it takes a few hard collisions to scale the barrier. Imagine a fast descent from a steep barrier. The rapidly descending system must, at the foothills, run into one or a few solvent atoms (Charutz and Levine 1993). Only if the coupling to the solvent is extremely effective (as if the solute is immersed in honey) the system will lose much of its energy while it is still descending. In the next section we will make this description somewhat more quantitative but the essential point should be recognized already here: on the time-scale of the descent from a typical chemical barrier, a typical weakly coupled solvent does not respond fast enough. The same considerations of microscopic reversibility also identifies the sub-group of those trajectories that start as thermal separated reactants and do cross the barrier as the entire set of trajectories that begins at the barrier and, when propagated backward in time, descends into the reactants region. As a practical point it is much more efficient to initiate MD calculations at the barrier top and propagate both forward and backward in time. In this way one generates only that subset of trajectories that do scale the barrier (Anderson 1973, 1975, Bennett 1977, Keck 1962, 1967).

5.4. *A model for activated barrier crossing in solution*

As argued in section 5.2 the minimal Hamiltonian that is needed to describe the short time-scale dynamics needs only to include the motion along the reaction coordinate, q, and a single solvent–solute effective coordinate, r. This involves the 2×2 sub-matrix of the full $(N+1) \times (N+1)$ matrix of equation (46). The two-dimensional model Hamiltonian

$$H = \left(\frac{m}{2}\right) \dot{r}^2 + \left(\frac{\mu}{2}\right) \dot{q}^2 + E(q) + \frac{k}{2}\left[r - r_e - \frac{C}{k}(q - q^{\ddagger})\right]^2 \tag{50}$$

couples linearly the two coordinates, and the two masses m and μ are important in determining the dynamics. $E(q)$ is the potential along the reaction coordinate, and $q^{\ddagger}$ is the position of the barrier. The linear coupling C and the harmonic force constant k result from the rotation transformation that we outlined in section 5.2. The former is just a sum over all the solvent modes to which the solute is effectively coupled, equation (48), while the latter is given by a weighted sum of the solvent force constants, equation (47). The coupling term C can also be shown to be related to the friction parameter γ that governs the overall rate of momentum dissipation in the Langevin equation. In practice we use the simulations to determine the force constants via the relevant dominant frequencies in the power spectrum. In this model the gas phase perpendicular degrees of freedom are ignored and the dissipation of energy from the reaction coordinates involves a solvent–solute motion. From the gas phase dynamics (Levine and Bernstein 1987, Smith 1980) we know that certain reactions exhibit a strong coupling between the reaction coordinate and the one perpendicular to it ($F + H_2$ is but one example). The role of this coordinate in the liquid (Charutz and Levine 1993) is still an open question.

Before proceeding to describe the results we wish to define the reduced parameters which govern the problem and explain the nature of the adiabatic procedure that will be employed. The reduced parameters are measured in units of the solvent–solute frequency ω, and its mass m. We therefore define a reduced coupling constant,

$$\gamma^* \equiv (\gamma/\omega) = (C/k)^2(m/\mu), \tag{51}$$

and a reduced local frequency along the reaction coordinate,

$$\rho^2(q) \equiv \omega^2(q)/\omega^2 = [K(q)/k](m/\mu). \tag{52}$$

The strength of the coupling γ is scaled by the frequency ω. Their ratio measures how promptly the solvent can respond to the changes in the solute. The higher the frequency the faster is the solvent response to the reactants motion along the reaction path. In the weak coupling limit (which is appropriate for inert liquids) $\gamma^* < 1$ and vice versa for strongly coupled solvents, such as protic ones capable of creating hydrogen bonds. The reduced local frequency $\rho^2(q)$, is the ratio between the reaction coordinate frequency and the solvent–solute frequency. Below we shall argue that it is the high value of $|\rho^2(q)|$ in and about the barrier to reaction that is the reason for the failure of rare gas solvents to effectively cage the reactants in the barrier region.

In the next section we discuss the adiabatic separation. We will take the adiabatic limit to be the one where the solvent is moving fast and is able to follow the motion along the reaction coordinate. The opposite is true in the sudden limit, where we have a fast motion along the reaction coordinate and a sluggish, slow, one along the solvent–solute mode. In both limits the solute can be strongly or weakly coupled to the solvent. The different limits (adiabatic, sudden and strong or weak coupling) were discussed in detail by van der Zwan and Hynes in their study on the isomerization of a dipole in a polar solvent (1982, 1983, 1984). The solvent response time-scale is determined not only by the potential. The masses can play a decisive role. A heavy solvent–solute particle will not be able to follow a light particle moving along the reaction coordinate. Thus the solvent can partially compensate for the disparity in force constants in the barrier region by a low inertia, i.e. $m < \mu$, but this, by itself does not imply a strong coupling between the two motions.

5.5. *Adiabatic separation*

The disparity between the solvent frequency and that of the motion along the reaction coordinate suggests that we introduce an adiabatic separation of coordinates. This is the exact analogue of the Born–Oppenheimer approximation, in which the fast motion is that of the electrons. This fast motion is able to adjust at every point in time to the instantaneous positions of the slow(er) coordinate(s). There are however two important points of difference. First, it is only near the barrier top that the motion along the reaction coordinate is faster than the motion of the solvent. This is no longer true at the foothills of the barrier so that non-adiabatic transitions will be important. The second, is an important family of reactions (typically, activationless processes, Ben-Nun and Levine 1994) for which the opposite is true, namely that in the region of the barrier to reaction it is the solvent motion which is faster. As we shall point out, one characteristic of this family is the strong solvation of the reactants (which is absent in weakly coupled solvents, such as rare gases).

The adiabatic procedure that we apply is based on a local harmonic approximation for estimating the time-scale of the motion along the reaction coordinate. We then examine its validity, and in particular its failure, and use it to explain the local energy exchange between the solvent and the solute. An adiabatic separation of variables is possible when one can neglect the local anharmonicity of the reaction coordinate potential. This enables us to diagonalize the coupling between the r and q motions via a scaling and a rotation (the scaling is needed to get a common mass for the kinetic energy term). The old coupled diabatic coordinate set is replaced by a new mass weighted adiabatic set and the Hamiltonian is written as a sum of uncoupled

quadratic terms. When the potential energy is not harmonic a separation of variables is, in general, not feasible, and therefore the key step to what follows is the local harmonic approximation and the magnitude of the anharmonic terms provides a measure to the validity of the separation. The local harmonic approximation is time dependent and therefore the adiabatic rotation angle θ, that transforms the original diabatic coordinates to the uncoupled adiabatic set, will depend on time. In the adiabatic approximation this time dependence is neglected and the kinetic energy is written as a sum of square terms using the two adiabatic coordinates Q and R

$$T = \frac{m}{2}(\dot{Q}^2 + \dot{R}^2), \quad \text{(adiabatic approximation)}. \tag{53}$$

The potential energy is written in a similar form using the two eigenvalues of the reduced local harmonic force constants matrix given by

$$\begin{pmatrix} \lambda_+(q) & 0 \\ 0 & \lambda_-(q) \end{pmatrix} = \mathbf{U}^{\mathrm{T}} \begin{pmatrix} \rho^2(q) + \gamma^* & \sqrt{\gamma^*} \\ \sqrt{\gamma^*} & 1 \end{pmatrix} \mathbf{U}, \tag{54}$$

where

$$\mathbf{U} = \begin{pmatrix} \cos\theta(q) & \sin\theta(q) \\ -\sin\theta(q) & \cos\theta(q) \end{pmatrix}. \tag{55}$$

The angle $\theta(q)$ is that required to diagonalize the Hamiltonian

$$\tan 2\theta(q) = \frac{2\sqrt{\gamma^*}}{\rho^2(q) + \gamma^* - 1}. \tag{56}$$

Note that just as in the corresponding Born–Oppenheimer problem the diagonalization procedure has eliminated the potential coupling at the expense of introducing coupling terms in the kinetic energy (Rebentrost 1981). In the adiabatic approximation these terms are neglected and thus the validity of the separation depends on their magnitude, and, in particular, on the time dependence of the rotation angle θ. When the angle is changing rapidly, the adiabatic separation is no longer valid.

The efficiency of energy transfer is related to the adiabatic parameter. The latter is given by the inverse of the reduced time dependence of θ (Ben-Nun and Levine 1992b)

$$\xi^{-1} = \left|\frac{\mathrm{d}\theta}{\mathrm{d}\tilde{t}}\right|. \tag{57}$$

Here $\tilde{t} = \omega t$ and ω is the solvent–solute vibrational frequency. The motion is adiabatic if $\dot{\theta}$ is small compared to the frequency of the r and q motions, i.e. when $\xi > 1$. In the non-adiabatic limit the angle is changing rapidly, $\xi < 1$, and the impulsive deactivation (or activation) process is efficient.

The minimum energy path for a model reaction is shown in the upper panel of figure 7. During most of the motion the adiabatic rotation angle is constant and only to the right and to the left of the ridge it is changing rapidly. It is at these dangerous regions, where the surface is curving, that the solvent–solute motion will couple to the reaction coordinate via a resonant local frequency matching that is shown in the lower panel of figure 7. Other than that the motion is in the weak coupling adiabatic limit and the separation of variables is *de facto* exact. The full MD simulations exhibit this local frequency matching as a large and rather impulsive energy transfer from the solvent to the solute as the latter is ascending the barrier, figure 8. Using time reversibility arguments (see previous section) one can equally well view this process as an energy transfer from the solute to the solvent as the former is descending from the barrier. The

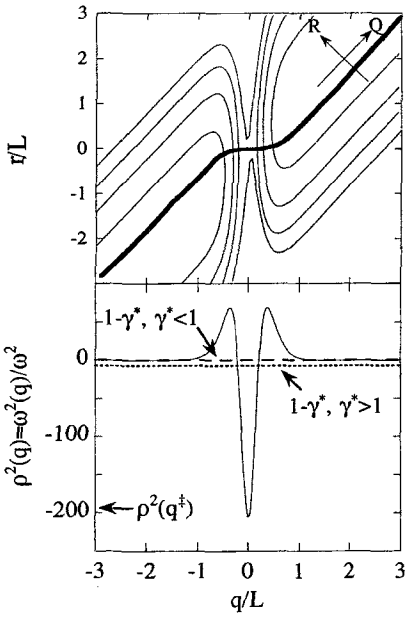

Figure 7. Upper panel: contour plot of the two-dimensional model potential energy surface for a symmetric ($A + BA$) atom exchange reaction. The minimum energy path is indicated by the thick line. The equipotential contours are 1·5 Kcal mol^{-1} apart. Note the short range of the barrier region, see figures 3 and 4. The rotation angle θ is defined as the local tilt of the adiabatic reaction coordinate Q with respect to the diabatic q axis, where q is the gas phase reaction coordinate. The value of θ serves as a measure for the solvent participation in the motion along the reaction path Q. Asymptotically, and at the barrier, θ is constant. (The asymptotic value of θ corresponds to the solvation of the reactants/products and as such it is not zero.) The rapid changes in θ occur at the foothills on either side of the barrier. When passing through such a region the adiabatic Q and R motions are no longer uncoupled. One can determine analytically that θ varies most with q at the point where $\rho^2(q_x) + \gamma^* = 1$. The position q_x where these localized non-adiabatic transitions take place is shown in the lower panel for the weak $\gamma^* < 1$ and strong $\gamma^* > 1$ coupling regimes.

same phenomenon was observed in the model Hamiltonian and is shown for an ensemble of model trajectories in figure 9. The motion down (or to) the barrier is essentially unperturbed and the reactants (or products) lose (or gain) all the available energy. Only when the foothills of the barrier is reached a vibrational non-adiabatic impulsive energy transition deactivates (activates) the products (reactants), the adiabatic separation breaks down and θ is changing rapidly. The energy transfer is impulsive and it is localized to positions q_x along the reaction coordinate where the two local frequencies match. For physical values of the friction term these transitions are confined to the foothills of the barrier. It is important to note that even though the results are for an average of 500 trajectories they all undergo activation (deactivation) at a similar time following the departure of the barrier at $t = 0$. In agreement with the full MD simulations the gas phase forces dominate in the barrier region and the solvent is actually frozen during the rapid crossing event (Ben-Nun and Levine 1992b, 1993a, Bergsma *et al.* 1986, Gertner *et al.* 1987, 1989, 1991, van der Zwan and Hynes 1983). Typical atom exchange reactions have a barrier with a rather short range, and hence the curvature of the potential is quite high. It therefore requires a very special solvent,

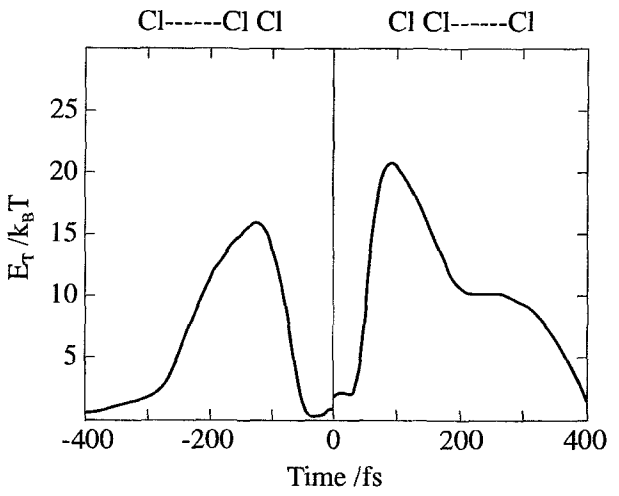

Figure 8. The kinetic energy for the relative motion of the reactants (negative times) and of the products of the symmetric Cl + Cl_2 atom exchange reaction in liquid Ar against time, in fs. The zero of time is when the system is at the saddle point. The temperature is 300 K and the reduced density is $\sigma^* = 0{\cdot}83$, molecular dynamics simulations of Charutz and Levine (1991a). In the gas phase, the relative kinetic energy will be constant both before and after the crossing of the barrier. It will only diminish during the very crossing as the kinetic energy is being used to surmount the potential hill. This is the case also in solution for the period of $\pm$ 100 fs during which the solute is essentially unperturbed. At longer times, energy exchange between the solvent and solute takes place. Before the collision, such an exchange is needed in order to activate the thermal reactants. After the collision, this exchange dissipates the energy released during the descent from the barrier (which is many times k_BT). As can be seen, this energy transfer is very impulsive. In one or two collisions with the solvent atoms the energy dissipation is essentially completed. This is more readily understood if we think of the descent from the barrier. As the products accelerate down the potential hill they run into a nearly stationary solvent atom, which serves to considerably slow them down. A similar behaviour is shown for the model Hamiltonian in figure 9.

with special properties, to be able to rapidly respond to this fast motion (Ben-Nun and Levine 1992b, 1993a). Quantitatively, the local ratio of the frequency along the reaction coordinate and that of the solvent-solute motion is a measure for that. In the fast solvent response regime $|\rho^2(q)| \leqslant 1$, but this only happens at the foothills of the potential. In the barrier region $|\rho^2(q)|$ is high and the solvent is frozen and unable to follow the solute motion. The dominance of the gas phase potential energy surface in the barrier region was observed even for model S_N2 reactions in water (Gertner *et al.* 1991).

It is helpful to think of the angle θ as a measure to the extent of solvation during the course of barrier crossing. The adiabatic approximation which assumes that the motion follows the instantaneous value of θ is thus the one where the solvation is rapidly adjusting, i.e., $(d\theta/dt)$ is negligible as compared to the solvent–solute frequency ω. One implication of the fact that the extent of solvation is measured by an angle is that one can shift θ by a constant angle θ_0 such that the reactants are not solvated (i.e., θ_0 is the value of the old θ as $q \rightarrow \infty$). Then the barrier in figure 7 would be tilted by an angle θ_0. Subtracting a constant angle does not affect the non-adiabatic coupling which depends on $(d\theta/dt)$. As is only to be expected, it does affect the rate of crossing of the transition state.

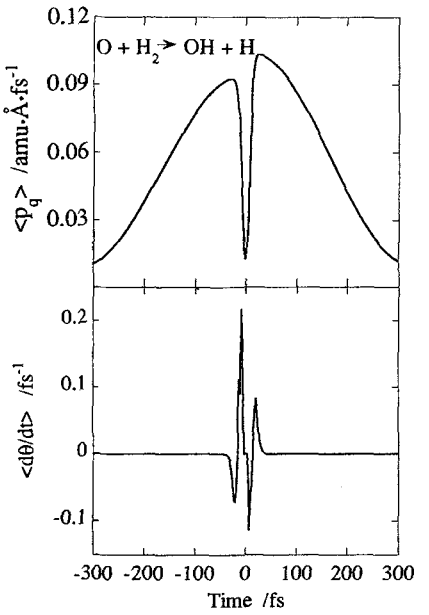

Figure 9. The momentum (upper panel) and non adiabatic coupling $d\theta/dt$ (lower panel) for an ensemble of 500 trajectories, computed for the model Hamiltonian, against time. The potential along the reaction coordinate is that for the $O + H_2$ reaction and the friction $\gamma^* = 0{\cdot}7$ is realistic for reactions in fluid Ar at 300 K and a reduced density of $\rho^* = 0{\cdot}83$. The trajectories are initiated at $t = 0$ from the top of the barrier with a thermal distribution in all the other degrees of freedom. Up to the crossing point q_x (where $d\theta/dt$ is extremal) the motion gains momentum due to the descent from the barrier. As a result of the non-adiabatic transition most of the barrier energy is converted to the r motion.

5.6. *Reaction rate*

For the separable Q and R motions the evaluation of the thermal TST rate constant is quite simple: it is a product of one dimensional partition functions

$$k_{\mathrm{TST}} = \frac{Q_R^{\ddagger}}{Q_R^{-\infty}} k_{\mathrm{TST1D}}. \tag{58}$$

Q_R is the partition function for the bound perpendicular adiabatic coordinate R which in the classical limit results in a one-dimensional vibrational amplitude

$$Q_R = (k_B T/\hbar\omega\lambda_+^{1/2}), \tag{59}$$

with $\omega\lambda_+^{1/2}$ being the frequency of the adiabatic R motion (calculated, as appropriate, for the reactants or at the TS), k_{TST1D} is the one-dimensional transition state theory rate constant for the unbound Q motion

$$k_{\mathrm{TST1D}} = (k_B T/h)(2\pi\mu kT/h^2)^{1/2} \exp[-E(q^{\ddagger})/k_B T]. \tag{60}$$

Here $E(q^{\ddagger})$ is the height of the barrier, and the pre-exponential factor is the de Broglie wavelength for the translational motion along Q times a frequency factor $k_B T/h$. In the absence of any solvent–solute coupling λ_+ equals unity and the TST result, equation (58), reduces to the one-dimensional limit, equation (60).

In the reduced description the effect of the solvent is described by a single phase space integral, equation (59). The solute particle is confined to an effective 'adiabatic'

free volume whose size is determined by summing over all the solvent–solute direct interactions, and by a weighted average over the normal modes of the solvent. This averaging is similar to the simplified result of cell theory, equation (24), in which the effect of the solvent–solvent interactions, and even more of that of the direct solvent–solute interactions was modelled via a single configurational integral. There is however a difference in the way that we interpret this effective free volume. Cell theory considers this volume to be a true physical cell in a geometric space whereas in the reduced model (and also in he 'exact' many-body result) the effective free volume corresponds to a normal mode of vibration and as such it exists in the more general phase space.

Equation (58) is also the reduced analogue of equation (22), in which the rate constant was written as a product of two disjoint manifolds of normal modes (one for the solvent and one for the solute and solvent–solute local modes), and a single correction term for the solvent modes. In the reduced picture the secondary solvent–solvent couplings (and hence their corrections) are neglected and account is taken only of the first manifold of normal modes that includes the solvated reactant and its direct coupling to the solvent via a single effective mode. We note however, that this effective mode does include in it all the solvent–solute interactions, see section 5.2. Thus the reduced rate constant, equation (58), may be viewed as the short time limit of the 'exact' many-body result of equation (22). It considers only the direct first-order solvent–solute interaction and the longer time-scale solvent–solvent interactions are neglected. (The geometric factor of equation (22) does not appear in the reduced two-dimensional model which does not include the rotational motion.)

The ratio of vibrational amplitudes, at the TS and for the reactants, that composes the deviations from the 1D result can be expressed as a scaling factor.

$$\begin{aligned} &= (Q_R^{\ddagger}/Q_R^{-\infty}) \\ &= (\lambda_+^{-\infty}/\lambda_+^{\ddagger}) \\ &= (1+\gamma^*)^{1/2}(k/m\omega^2\lambda_+^{\ddagger})^{1/2}. \end{aligned} \tag{61}$$

The second term in the last line is written so as to emphasize that it is the ratio of force constants (or of frequencies) for the motion perpendicular to the reaction coordinate without and with the coupling, and the first term is the correction for the solvation of the reactants. As argued before, due to the high curvature at the barrier to reaction (when compared to a typical solvent–solute interaction) the Q and R motions are effectively uncoupled in the barrier region. This suggests that in agreement with the MD simulations in which recrossing of the barrier were shown to be negligible at regular densities, the TS result, equation (58), provides a realistic estimate of the reaction rate so that the second correction factor of equation (58) is roughly one.

5.7. *Caging*

Caging is a short-time phenomenon that takes place when collisions with the solvent first solvation shell changes the sign of the momentum of the motion along the reaction coordinate. Caging can occur both before and/or after the crossing of the activation barrier. In the latter case, the products can remount the potential barrier and they may even succeed to recross back into the reactants region. On a longer time-scale, energy flows out of (or into) the first solvation shell into (or out of) the bulk of the solvent with the result that the reactants are thermalized or, if they attract one another they can also be stabilized (Ben-Nun and Levine 1993c, 1994) as a bound pair. This energy relaxation

is, in weakly coupled solvents, slower then the vibrational motion in the cage. This hierarchy of time-scales was already noted in connection with equation (49) and earlier in the factorizations of the type (19).

In agreement with the full MD results (Ben-Nun and Levine 1992b) caging takes place only at such high densities that the friction (or coupling in our mechanical terms) is much higher, figures 10 and 11. The trajectory then recrosses the transition state and every recrossing is accompanied by a vibrationally non-adiabatic impulsive energy transfer at either side of the barrier. These recrossings of the TS reduce the net rate of reaction below the rate computed by TST for the crossing of the activation barrier. The magnitude of the correction has been discussed in section 3.3. The mechanical origin of the cage is clear when one examines the model potential along the reaction coordinate for different values of the coupling. As shown in the lower panel of figure 12, when the coupling to the solvent is strong (typically $\gamma^* > 1$ would suffice but the specific value does depend on the height of the barrier to reaction) the potential along the reaction path has a double well that results in a caged motion, due to the non-adiabatic transitions. For a 'clamped nuclei' discussion of caging see Patron and Adelman (1991).

It is interesting to note that for highly asymmetric reactions the criteria for caging for the forward reaction (reactants $\rightarrow$ products) need not necessarily be as the one for the reversed reaction (products $\rightarrow$ reactants). Such an extreme example is shown in the upper panel of figure 12 for the exchange reaction $F + H_2 \rightarrow FH + H$. For the specific choice of coupling that is shown ($\gamma^* \approx 2$) the reactants are already caged, as reported by Charutz and Levine (1993), yet caging for the products requires a somewhat higher value of the coupling to the solvent. When the value of the friction is high, i.e., $\gamma^* > 1$, the non-adiabatic transitions can take place closer to the barrier region, where the curvature $\rho^2(q)$ is still negative.

Note that not every trajectory must successfully recross the barrier. As mentioned earlier the reactants motion along the barrier is fast and the solvent may not be able to reorganize and facilitate the recrossing of the barrier. When the solvent does not have the time to adjust and re-optimize the transition state configuration the trajectories which are caged at the foothills of the barrier and are reactivated are then reflected from the top of the barrier. It is important to note that in the adiabatic limit the solvent–solute motion is able to follow the motion along the reaction coordinate, i.e., the r and q motions are synchronized. An unfavourable configuration of the transition state is a diabatic effect and it reflects a non-equilibrium configuration of the transition state. For many years people have looked for the Kramers fall-off regime (Hynes 1985b, Kramers 1940, Schroeder and Troe 1987, Tucker *et al.* 1991) where the rate constant is reduced due to frequent recrossings of the barrier. People often talked about a diffusive random walk motion along the barrier. The activated problem does not exhibit this Brownian motion-like behaviour as the typical barrier is rather high, short ranged and with a fairly high curvature. Caging, confined to the very top of the barrier region is our analogue of the Kramers over damped regime. It typically happens only when the coupling is strong, e.g., $\gamma^* > 1$ (so that the range of the cage is limited, see figure 12) and it requires that the coupling as measured by $\gamma^*/[-\rho(q)]^2$ is not small.

5.8. *Separation of time-scales*

We study the separation of time-scales using the complementary frequency domain. First, we wish to emphasize that this separation is due to a large difference in the magnitude of the reduced parameters for the different locations along the reaction coordinate and that the different time domains can be discerned both in the full MD

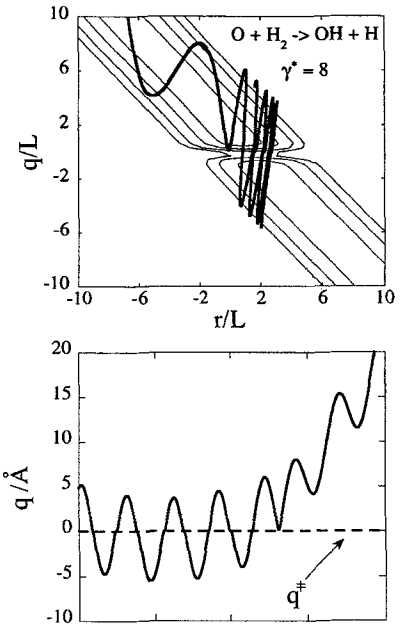

Figure 10. Upper panel: a caged trajectory for the O + H_2 reaction, computed using the model Hamiltonian, superposed on the potential energy surface at a high value of the reduced friction which corresponds to liquid Ar at a high density, see figure 12. The lower panel shows the actual trajectory as a function of time. The repeated crossings of the barrier can be identified as due to strong non-adiabatic transitions in the vicinity of the barrier.

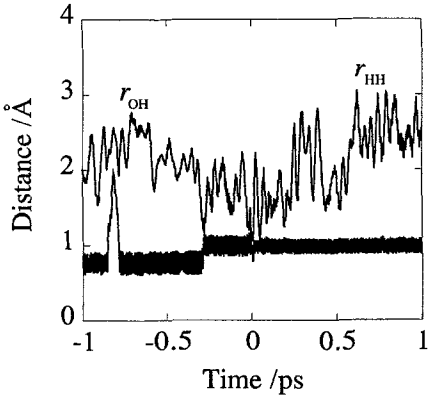

Figure 11. A full MD calculation for the O + H_2 reaction in fluid Ar at a high reduced density of $\rho^* = 1{\cdot}68$. At this density the solvent atoms themselves are caged, see figure 6. Shown are bond distances against time. Note the many attempts, some successful, to recross the barrier. This breakdown of the transition state approximation is due to the caging at the foothills of the barrier, see figure 12. When such a caging is possible, one should use the modification discussed in section 3.3, which takes the cage motion into account. Note the time scales here and in figure 5. The caged motion occurs in the sub ps time regime.

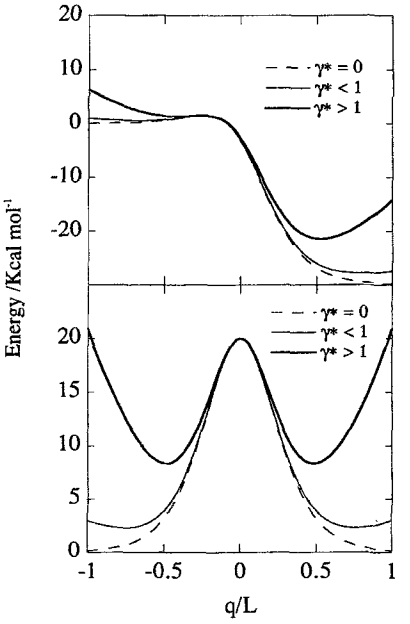

Figure 12. The potential along the reaction coordinate for different values of the coupling to the solvent for a symmetric (lower panel) and asymmetric (upper panel) reaction. In both panels the dashed line is the potential for the bare reactants i.e., the coupling to the solvent is zero. The full lines correspond to the weak ($\gamma^* = 0{\cdot}7$, thin line) and strong ($\gamma^* = 1{\cdot}8$, thick line) coupling regimes. Lower panel: the symmetric Cl + Cl $_2$ reaction. The caged motion is seen to be a result of the double well potential along the reaction coordinate that is present when the coupling to the solvent is large. The motion is then caged and the trajectories recross the TS, see figures 10 and 11. (As is only to be expected the specific value of γ^* needed to induce a caged motion would depend on the height of the activation barrier to reaction. The larger is γ^*, the more confining is the cage.) Upper panel: the highly asymmetric F + $H_2 \rightarrow$ FH + H reaction. As in the lower panel the increased coupling to the solvent results in a double well along the reaction path however, due to the high asymmetry of this reaction the coupling needed for caging in the forward direction (i.e., reactants $\rightarrow$ products) is higher than for the reverse reaction (products $\rightarrow$ reactants). For this specific example the reversed reaction is caged yet stronger coupling to the solvent is required to induce caging in the forward direction. Note how in both panels the volume of the cage decreases as the coupling increases thus leading to a higher caging frequency, see figure 14 below.

simulations and in the reduced model. In and about the barrier region it is the bare gas phase potential surface that is dominant, see figures 3 and 4. Thus the fast crossing event is essentially unperturbed and is similar in many ways to the gas phase problem.

The energy of a stationary quantum oscillator is well defined and therefore its phase is random. For a non-stationary oscillator this need not be true. It can have a spread in its energy with the result that its phase is well defined and thus it can be viewed as a classical particle oscillating in its well. For an A + BC reaction a classical ensemble of outgoing AB product molecules does not have a sharply defined energy and therefore its phase may be localized. The vibrational motion of the product molecule is perpendicular to the reaction coordinate, and the reduced model ignored it. Unlike the familiar continuous wave spectrum, the absorption spectrum of such an ensemble will oscillate with a frequency that is similar to the vibrational frequency of the

perpendicular degree of freedom (provided that the duration of the light pulse is shorter than the probed frequency). If this coherent vibrational motion of the perpendicular degree of freedom prevails for a long enough period it can be probed by fast (femto second) lasers. Recent ultrafast optical pumping experiments, both in the gas phase (Dantus *et al.* 1989, Khundkar and Zewail 1990, Mokhtari *et al.* 1990, Nelson and Williams 1987, Pollard and Mathies 1992, Rosker *et al.* 1988, Wise *et al.* 1987, Zewail 1991) and in condensed phase (Banin *et al.* 1992, Banin and Ruhman 1993, Fei *et al.* 1992, Scherer *et al.* 1993, Yan *et al.* 1992, Zadoyan *et al.* 1994, Zoval and Apkarian 1994) demonstrated an experimentally observable coherence in barrier descent dynamics. In the present study we regard the atom exchange reaction as a half collision: $ABC \rightarrow AB + C$. A swarm of classical trajectories is initiated from the saddle point region at $t = 0$ with all other coordinates and momenta chosen from a thermal distribution. Thus the trajectories are initiated from the saddle but with the most uniform distribution in all other degrees of freedom. The electronic absorption spectrum is calculated by invoking the Franck–Condon assumption (this assumption is convenient but not essential), and the resulting ultraviolet (u.v.) absorption spectrum corresponds to a bound to free transition of the AB molecule. Unlike the standard theory (Lax 1952) we use a probe field that is localized in time with an envelope centred at time t. The result is a time and frequency resolved absorption spectrum $I(\upsilon, t)$. Different reactions at different conditions were studied, here we refer to the symmetric $Cl + Cl_2$ reaction in the gas phase and in liquid Xe (Ben-Nun and Levine 1993b). Both in the gas phase and in the liquid the initial evolution of the density did not spread out to uniformly sample the available phase space. Rather, over a time interval that can be probed using ultra-fast spectroscopy, it remained localized in phase space and hence exhibited a coherent motion, figure 13. At a longer time scale (> 500 fs), the coherence decays primarily due to intramolecular anharmonicity and not, as might be expected, due to coupling to the solvent. Moreover, the initial caging by the solvent seems to reduce the initial dephasing. To study the role of the tight transition state in inducing this coherence we have 'opened it up' by raising the transition state temperature to the (physically non-realistic) value of 3000 K. At this high temperature all other coordinates and momenta span a wider range, and as a result there is no coherence in the spectrum. Thus the inability of the solvent to compete with the gas phase potential energy forces is manifested in the perpendicular degree of freedom: both in the gas and in the liquid the action variables (which are conjugated to the phase) are distributed non-uniformly, they dephase due to intramolecular anharmonicity which is faster then intermolecular solvent dephasing (Oxtoby 1981).

At a longer, yet sub-picosecond, time-scale the fairly frequent collisions with the liquid atoms detain the products (and/or reactants) at the distant foothills of the activation barrier (Ben-Nun and Levine 1992b). These repeated collisions with the rare gas atoms (lower panel figure 14) generate a collision induced spectrum in the far infrared (i.r.) region (Ben-Nun and Levine 1993a). (The semiclassical spectrum is computed by calculating the Fourier transform of the dipole moment function, and the time dependent value of the dipole is calculated from classical MD trajectories (Koszykowski *et al.* 1982, Papoulis 1962).) Whether or not these collisions result in re-crossings of the barrier we refer to them as a caged motion as they confine the reactants to the region of chemical forces. In other words, we make a distinction between the classical cage effect (Hynes 1985b, Kramers 1940) in which the reactants (or products) are made to retrace their descent and re-scale the barrier and the more general notion of a caged motion. In the latter case the reactants (or products) are

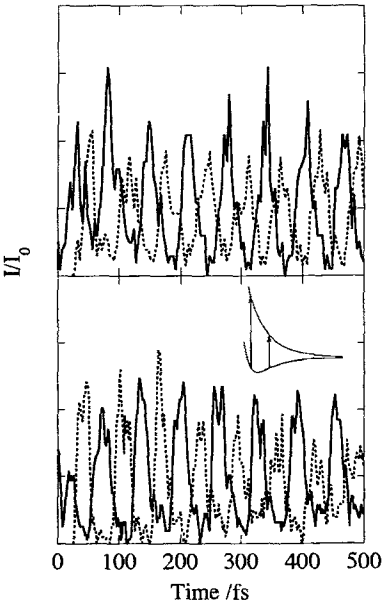

Figure 13. The time dependence of the ultrafast probe absorption spectrum at lower (dashed line) and higher (solid line) frequencies. The solid (dashed) line corresponds to a vertical transition near to the outer (inner) turning point. Upper panel: $Cl_3 \rightarrow Cl_2 + Cl$ in the gas phase; dashed line 45 000 cm^{-1}; full line 75 000 cm^{-1}. Lower panel: same reaction in liquid Xe. Computed using a full MD simulation at a reduced density of 0·83; dashed line 45 000 cm^{-1}; full line 85 000 cm^{-1}. As would be expected for a fully coherent motion the time dependence of the two spectra is exactly out of phase and the period is essentially that of the vibrational motion of Cl_2.

detained for a measurable duration at the foothills of the barrier. The upper panel of figure 14 shows a distinct frequency of the solvent–solute motion that is far lower then the frequency of the OH–H or H–H chemical bond.

The well defined power spectrum of the caged motion also serves to validate our conclusion that in weakly coupled solvents, the deactivation of this motion, by energy transfer to further removed motions of the solvent, is a slower process. We next turn to a different situation where both because of longer-range attractive forces between the reactants and due to strong coupling to the solvent, the caged motion is heavily damped.

6. Actionless processes and the role of solvation

We next proceed to discuss an ion–molecule activationless recombination process in a solvent of structureless atoms. Attention is centred on the dynamics of the motion into the polarization well (Adams *et al.* 1983, Barlow *et al.* 1986, Ferguson 1974, Lim and Brauman 1991, Olmtead and Brauman 1977, Pellerite and Brauman 1980, Rabani *et al.* 1991) and we do not address the crossing of the chemical barrier which lies closer in than the polarization well. Hence, the molecular dynamics simulations are aimed to mimic a capture process in solution. Here too we will invoke an adiabatic separation of variables and examine the validity of simple gas phase models, such as the capture model, in solution.

As in the gas phase the two classes of reactions (activated (Levine and Bernstein

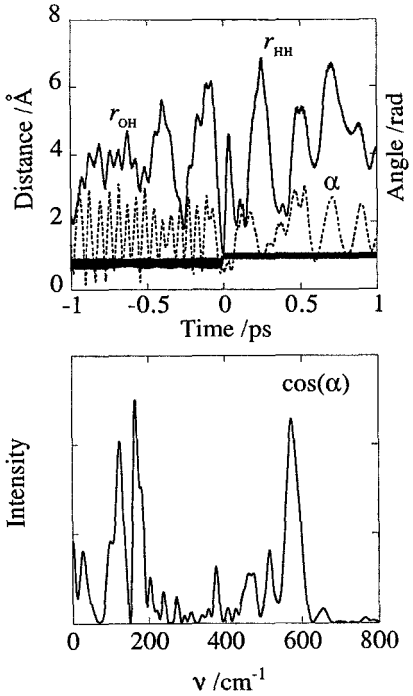

Figure 14. Upper panel: A reactive trajectory for the $O + H_2 \rightarrow OH + H$ reaction in fluid Ar at a reduced density of 0·83 and 300 K. The two bond distances (full line) and approach angle α, see insert figure 5, are shown against time. This typical trajectory approaches the barrier (and crosses it rapidly) only once. The reactants (products) spend a considerable time within a joint solvation shell, at the distant foothills of the activation barrier to reaction, due to frequent collisions with the liquid atoms. Lower panel: The power spectrum of $\cos\alpha$ against frequency. The frequent collisions with the solvent atoms generate a collision induced spectrum in the far i.r. region. By restricting the time integration of the Fourier transform to positive or negative values only, we identify the higher pick at 585 cm^{-1} to be due to the motion of the reactants (with respect to the solvent) while the lower frequency peaks are due to the relative solvent-products motion.

1987, Smith 1980) and activationless (Bagchi and Fleming 1990, Ben-Amotz and Harris 1987, Clary 1990, Keirstead *et al.* 1991)) serve as opposite models to simple bimolecular reactions. The first category, which we already discussed, will typically involve a reaction between neutral atoms or molecules whereas the second category, to which we next refer, includes radical recombination, ion–molecule reactions and exchange reactions between polar reactants (Schroeder and Troe 1987, Bagchi 1989). As we move from the activated problem to the activationless one we will show that, at the bottleneck to reaction, the nature of forces changes and even reverses. The reason is that in the absence of an intrinsic barrier to recombination, the only barrier to reaction, in the gas phase, is due to the rotational motion of the approaching reactants (Levine and Bernstein 1987). (The recombination of two methyl radicals (Eyring *et al.* 1936, Goring 1938) is but one example of a reaction with a rotational barrier.) The position of this rotational barrier is at a large ion–molecule separation (Levine and Bernstein 1987, Smith 1980) (when measured in units of the ion–molecule interaction length-scale σ). At this large separation the reactants are attracted only by their mutual long-range attractive interaction whereas the ion is solvated by the liquid first solvation shell. There

are two unrelated, different, reasons why the activationless process is so different from the previous problem: (1) the reactants' long-range interaction is physical and is therefore not comparable to a chemical interaction, and (2) the interaction with the solvent is different. We have an ion or a polar reactant which at room temperature is typically bound to one (or more) liquid atoms and the two are vibrating (and possibly rotating) around their equilibrium distance. This simple observation is shown in figure 15 where we plot the polarization potential of the reaction coordinate along with its local frequency measured in units of the ion–solvent equilibrium frequency, (k/m). In and about the rotational barrier region the solvent is moving faster than the slowly diffusing reactants (in our notation this is noted by $\rho^2(q) < 1$). Only to the left of the rotational barrier near the equilibrium distance do the reactants feel a strong chemical attraction. This disparity in forces governs the different major aspects of the recombination dynamics which we next describe.

Molecular dynamics trajectories of a model ion-structureless molecule recombination in an atomic solvent show a strong ion–solvent relative interaction (Ben-Nun and Levine 1993c, 1994). This strong attraction is manifested in the time dependence of the ion–molecule rotational quantum number. In contrast to the gas phase problem where it is constant (Levine and Bernstein 1987) here it is changing rapidly and with a frequency that is similar to the ion–solvent vibrational frequency, figure 16. This correlation may be checked by comparing the frequency of the Fourier transform of the ion–solvent distance to that of the ion–molecule rotational quantum number, or by running the dynamics with but one liquid atom and noting that when the latter is not bound to the ion the ion–molecule rotational quantum number is essentially constant (Ben-Nun and Levine 1994). The large alteration of the ion–reactant molecule rotational quantum number j suggests that one ought to re-examine the usual procedures which are ordinarily invoked when calculating a thermal rate constant: thermal averaging of the j dependent rates (Borkovec and Berne 1986, Straub *et al.* 1986) or using a single rate calculated using a j averaged effective potential (Sceats 1986). (The effective potential is a sum of the attractive potential energy and the repulsive kinetic energy term associated with the rotation of the relative motion of the reactants (Levine and Bernstein 1987).)

The MD simulations have further pointed to the possible formation of a 'solvent-separated' ion-pair (Ciccotti *et al.* 1990, Rey and Guàrdia 1992, Winstein *et al.* 1954). At a large ion–molecule relative separation a solvent 'atom' can fit in between the two reactants. The formation of an ion–molecule pair is then delayed and it requires the reorganization of the solvent. As the ion–solvent separation decreases, two interactions are increasing and they both 'push' the solvent atom to the other side of the ion: the ion–molecule *attraction* is increasing and the molecule–solvent atom *repulsion* is increasing. Thus at a large ion–molecule distance the energetically stable configuration is ion–solvent–molecule and as the ion–molecule separation continues to decrease the most stable configuration becomes ion–molecule–solvent. The formation of a 'solvent-separated' ion pair was observed in molecular dynamics simulations of recombination dynamics of Br_2^- in clusters of Ar and CO_2 by Amar and Perara (1989, 1991). Experimentally, Lineberger *et al.* (Papanikolas *et al.* 1991, 1992) indicated that the formation of a 'solvent-separated' ion pair is actually feasible. In addition, once it is formed the ion–molecule pair can be stabilized by collisions with the solvent. In the gas phase an attempted recombination process of two structureless reactants ends in their final ultimate separation, due to conservation of energy. Hence, one needs a chaperon or a third atom for a successful capture (Smith 1980). The presence of the

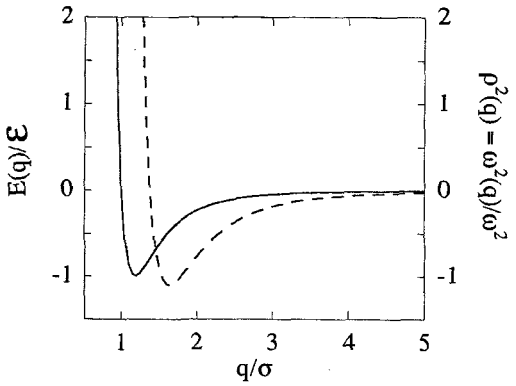

Figure 15. The ion–molecule polarization potential $E(q)$ (solid line) and its second derivative (dashed line) plotted in reduced units against the reaction coordinate q. ε is the ion–molecule well depth and ω is the frequency of the ion–solvent motion. The right ordinate shows $\rho^2(q)$, $\rho^2(q) = [K(q)/k][m_3(m_1 + m_2)/m_1(m_2 + m_3)]$. At large q values the force constant k for the solvation of the ion is larger than $K(q)$. Unlike the case for activated reactions, see figure 4, at and about the barrier in the effective potential ($= E(q)$ + centrifugal term), $\rho^2(q) < 1$. The difference is due to the location of the barrier in the effective potential which occurs for $(q/\sigma) > 1$.

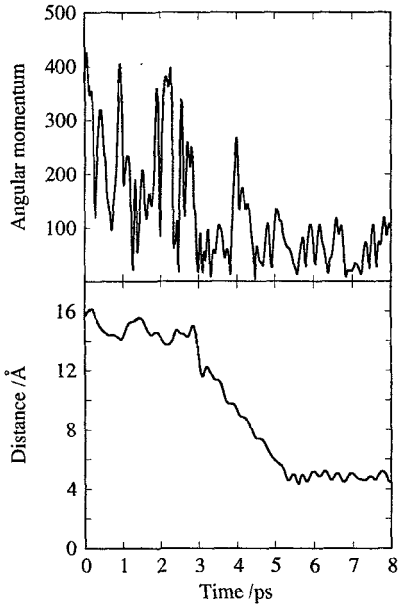

Figure 16. A typical molecular dynamics trajectory for the recombination of a Cl^- ion and a structureless CH_3Cl molecule in liquid Ar. Lower panel: the ion–molecule relative separation against time in ps. Note the capture into the polarization well at longer times, due to efficient stabilization of the ion pair by the solvent. Upper panel: the angular momentum j (in units of $\hbar$) of the approach motion against time. The gas phase capture model assumes that j is constant during the crossing of the centrifugal barrier. Here, due to the relative motion of the solvent with respect to the reactants (and particularly with respect to the Cl^- ion), j is constantly changing.

liquid provides this channel for energy dissipation, if energy transfer to the ion–solvent mode is efficient. Below we will use an adiabatic separation of variables to identify the point in time that gives the major contribution to this energy transfer.

6.1. *Model.*

The activationless model Hamiltonian (Ben-Nun and Levine 1993c) is similar in spirit to the activated one, yet there are some major differences. First, the present problem has an additional degree of freedom which was observed to be important in the full dynamics. Second, since we use a Cartesian coordinate system there is a kinetic coupling term, the last term in equation (63) below. Third, we use a nonlinear space dependent coupling term (Haynes *et al.* 1993, Krishan *et al.* 1992a, b, Strauss *et al.* 1993, Voth 1992). Depending on the masses involved, the kinetic coupling term can be significant and below we show that, for our choice of masses, it is the kinetic coupling term that plays the major role and not the potential coupling. However, the nonlinear potential energy coupling term is essential to our model as it mimics the reorganization process of the solvent.

The relevant coordinates in the recombination process are the ion–solvent coordinate $\mathbf{r}$ and the ion–structureless molecule relative coordinate $\mathbf{q}$. Using a vector notation for both $\mathbf{r}$ and $\mathbf{q}$, the angle α between them does not show explicitly. Thus the three dimensional model Hamiltonian

$$H \equiv T + V(\mathbf{r}, \mathbf{q}), \tag{62}$$

where

$$T = \frac{1}{2}\frac{m_1(m_2+m_3)}{M}\dot{\mathbf{q}}^2 + \frac{1}{2}\frac{m_3(m_2+m_1)}{M}\dot{\mathbf{r}}^2 - \frac{m_1 m_3}{M}\dot{\mathbf{r}}\cdot\dot{\mathbf{q}}, \tag{63}$$

$$V(\mathbf{r}, \mathbf{q}) = E(\mathbf{q}) + \frac{k}{2}\left(\mathbf{r} - \mathbf{r}_e + \frac{C(q)}{k}\mathbf{q}\right)^2 \tag{64}$$

has two coupling terms. In equation (63) m_1, m_2 and m_3 are the ion, molecule, and solvent atom masses, respectively and M is the sum of masses. The long-range part of the polarization potential along the reaction coordinate $E(\mathbf{q})$ has a q^{-4} dependence, k is an ion–solvent harmonic force constant (estimated using the same methods described in the activated problem), and $\mathbf{r}_e$ is the ion–solvent equilibrium distance (estimated also from the full MD simulations). The potential coupling term $C(q)$ is introduced to mimic the solvent reorganization process and its functional form is determined as follows. At a very large ion–molecule separation the ion and solvent are vibrating and rotating freely (in the solvent this rotation may be hindered by the other neighbouring solvent atoms), the coupling to the reaction coordinate is then only due to kinetic coupling (last term in equation (63)). As the ion–molecule relative separation decreases the potential coupling changes from zero. Its sign is determined by the requirement that at a large separation the stable configuration is molecule–solvent atom–ion. A further decrease in the relative separation results in a change of sign of $C(q)$ that enables the reorganization of the solvent. The position where the sign changes is estimated from a fit to the three-body potential used in the MD simulations, and the length scale is chosen to ensure a smooth but rather abrupt change of sign.

Figure 17 shows an example of a model Hamiltonian trajectory. There are two important points to note in this trajectory. One is that in agreement with the full MD simulations (figure 16), the angular momentum, j, of the ion–molecule relative

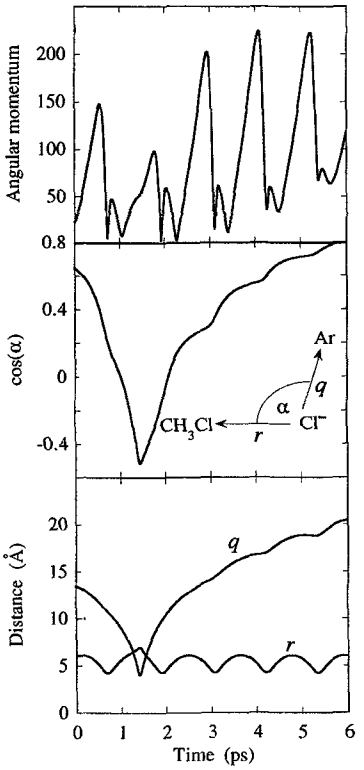

Figure 17. A model Hamiltonian trajectory for a chaperoned encounter between a Cl^- ion and a CH_3Cl molecule. A single Ar atom is solvating the ion. Bottom panel: the ion–molecule (q) and ion–solvent (r) distances against time in ps. Middle panel: the orientation of the chaperon Ar with respect to the ion–molecule axis. Initially the Ar atom was in the way as the stable configuration is ion–solvent atom–molecule. As the ion–molecule relative separation decreases the solvent atom rotates to the other side of the ion and thus enables the recombination to proceed. Upper panel: the angular momentum j (in units of $\hbar$) of the ion–molecule relative motion. In agreement with the full MD simulations, see figure 15, the angular momentum is changing with a frequency that is evidently similar to the frequency of the ion–solvent atom relative motion.

separation is changing rapidly and with a frequency that is evidently similar to the ion–solvent vibrational frequency. The second point is the formation of a 'solvent-separated' ion-pair which is followed by a solvent reorganization process. At $t = 0$ the chaperon solvent atom is placed randomly around the ion and the stable configuration is ion–solvent atom–molecule. As the ion–molecule relative separation decreases the solvent atom is rotating to the other side of the ion and thus enables the recombination to proceed. Note that despite the extensive energy exchange the solvent did not drain enough energy from the reaction coordinate and the trajectory results in the final separation of the structures reactants.

6.2. *Ion-pair stabilization*

It is often the case, both in the full MD and in the model, that the newly formed species undergoes an efficient vibrational stabilization process (Ben-Nun and Levine 1993c, 1994). This is in contrast to the gas phase where the only possibility of vibrational

deactivation of two structureless particles is that of an inefficient radiative decay. The presence of the liquid, or of any other additional degree of freedom, opens a new channel for energy dissipation. Experimentally the vibrational relaxation is studied by selectively exciting a vibrational level using i.r. absorption or stimulated Raman scattering and then studying the vibrational relaxation by monitoring the recovery of the i.r. active transitions, by time and frequency resolved fluorescence or by direct optical detection (Chesnoy and Gale 1988, Graener *et al.* 1989, Harris *et al.* 1990, Laubereau and Kaiser 1978, Smith and Harris 1990). When there can be a frequency matching between the solvation coordinate and the solute vibrational coordinate the reported (Brown *et al.* 1988) time-scales range from 1 to 100 ps, depending on the strength of the solvent–solute interaction. Molecular dynamics simulations show similar results (Benjamin and Whitnell 1993, Staib and Hynes 1993).

The present study of the deactivation process is motivated by the mechanical description of the system, i.e., the Hamiltonian in equation (62). An adiabatic separation of variables is used to study the efficient V–T energy transfer. The adiabatic separation is similar to the one used in the activated problem, the only difference here is that both the kinetic and the potential energy have to be diagonalized simultaneously. Just as in the former problem, the procedure is based on a local harmonic approximation of the polarization potential along the ion–molecule relative separation coordinate. Once the potential energy is written in a quadratic form we use the **FG** procedure of molecular spectroscopy (Wilson *et al.* 1955) and simultaneously diagonalize both the kinetic and the potential energy. The end result is a set of new adiabatic vectors **Q** and **R**. The new vectors are a linear combination of the old ones. Just as in the former problem the exact dynamics need not necessarily be in the adiabatic limit. In particular we will examine the breakdown of this separation. The sticky collision which is shown in figure 18 demonstrates the efficient coupling between the two modes that leads to the formation of a rather long lived complex. Note that as emphasized before, most of the motion is in the adiabatic limit. This is indicated by a constant value of the adiabatic angular momentum (see next section) and the adiabatic rotation angle θ. The sudden changes in θ are localized in time. They occur while the reactants are inside their well and correspond to energy exchange between r and q. The repeated collisions enhance the V–T energy transfer and are hence analogous to the role of van der Waals bound species (Ewing 1978) in gas phase V–T energy transfer. Thus the ion–solvent first solvation shell provides the necessary coordinate that can effectively couple to the vibrational motion of the highly excited ion–molecule pair and stabilize it for long periods.

6.3. *Constants of motion*

The possibility of a reduced description of liquid phase dynamics and in particular the idea of extending gas phase models to solution has been the aim of much theoretical research. For example, Wilson *et al.* (Li and Wilson 1990) examined the validity of Polanyi's rule in solution, i.e., the correlation between the location of the barrier along the reaction coordinate and the energy requirements and/or disposal in the reaction. They found that for the symmetric $Cl + Cl_2$ activated exchange reaction, in a rare gas solvent, there is a time duration of $\pm$ 100 fs around the barrier for which the gas and liquid phase energy partitioning is similar. Just as in the gas phase problem, an early barrier along the reaction coordinate leads to a preferential energy release to the vibrational motion of the product molecule. Thus for the case of an activated reaction in a weakly coupled solvent there is a short, yet experimentally detectable, time duration (confined to the barrier region) for which the gas and liquid phase dynamics are similar.

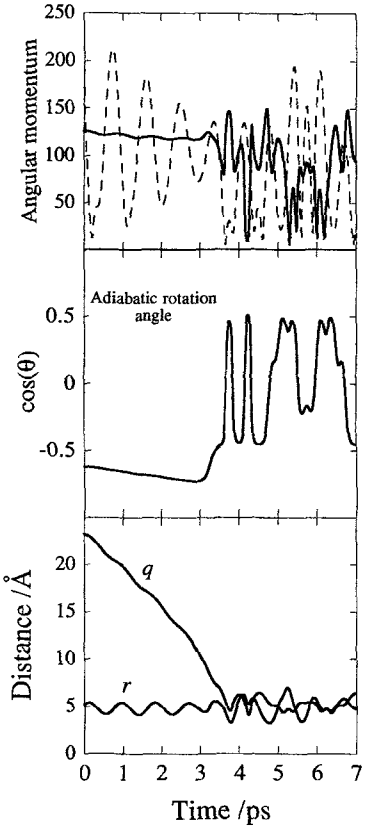

Figure 18. A model trajectory for the activationless recombination reaction. Lower panel: as in figure 17 the two bond distances against time. Middle panel: the adiabatic rotation angle θ. The efficient energy transfer to the solvation mode results in the formation of a stable adduct. (Figure 16 shows a similar phenomenon for the full MD simulations.) Upper panel: the diabatic (dashed line) and adiabatic (solid line) angular momentum (in units of $\hbar$) of the ion–molecule separation q against time. The angular momentum of the adiabatic reaction coordinate Q is essentially constant during the crossing of the effective barrier to reaction whereas, in agreement with the full MD results (figure 16) the diabatic angular momentum j is constantly changing. The constant value of the adiabatic angular momentum enables us to extend the gas-phase capture model to solution.

Charutz and Levine (1991a, b, 1992) have discussed the more general problem of how to dress the gas phase variables (i.e., to solvate them) such that the new dressed variables satisfy the gas phase equations of motion. Below we discuss a more approximate approach where the variables are only useful in the adiabatic limit. We illustrate the idea by a specific application, that of deriving a capture model for activationless reactions.

The capture model (Levine and Bernstein 1987, Clary 1990, Smith 1980, Smith *et al.* 1989) has been used for many years to estimate the gas phase reaction rate or capture cross section. The model is based on the notion of an effective potential which is the sum of the attractive potential energy and the repulsive kinetic energy term associated with the rotation of the relative motion of the reactants. (The repulsive kinetic energy term keeps the two colliding particles apart.) Thus at large separations the effective potential has a barrier and its position and height are energy dependent (it shifts

closer in for higher collision energies). By adding the centrifugal term to the long-range attractive potential (the short-range repulsion is neglected) the position and height of the effective potential is evaluated and one assumes that if the particles cross this point reaction proceeds with a unit probability. This rather naive model oversimplifies the problem by neglecting many effects (such as steric requirements (Jensen 1992, Levine and Bernstein 1988, Turulski and Niedzielsky 1988, Rabani *et al.* 1991), the role of reactants vibrational excitation (Hase *et al.* 1992, Troe 1987, 1989, Tucker and Truhlar 1989, Vande and Hase 1990) etc.), yet it is able to predict trends and systematics. For example, for ion–molecule reactions (an r^{-4} attractive potential) it is found that, unlike the case of an activated reaction, the reaction cross-section decreases as the relative kinetic energy increases and the chemical rate constant is temperature independent (Gioumousis and Stevenson 1958). To be able to apply the capture model in solution an effective constant angular momentum has to be found (Ben-Nun and Levine 1994). One can then predict the final outcome of a trajectory just by looking at the initial constant value of the relative adiabatic angular momentum.

By applying the adiabatic procedure both the kinetic and the potential energies are separable and we can then define a constant angular momenta along the two adiabatic coordinates **Q** and **R**

$$\left.\begin{aligned}\mathbf{J_Q} &= \mathbf{Q} \times \dot{\mathbf{Q}},\\ \mathbf{J_R} &= \mathbf{R} \times \dot{\mathbf{R}}.\end{aligned}\right\} \tag{65}$$

Note that equation (65) is correct only in the adiabatic limit, i.e., when the time dependence of the rotations that diagonalize the Hamiltonian of equation (62) is neglected. The upper panel in figure 18 shows that the separation of variables is exact for most of the motion and in particular for the region of interest, i.e., about the centrifugal barrier to reaction. Only after the particles have crossed the barrier and have approached each other to well within the range of their chemical forces does the adiabatic separation break down. The breakdown of the adiabatic separation is confined to the region of chemical interaction and it is manifested by the rapid changes of the adiabatic angular momentum. The outcome of a trajectory can now be predicted by examining the initial value of the adiabatic angular momentum along the adiabatic reaction coordinate. If this value is too large the colliding particles do not cross the centrifugal barrier to reaction, and the trajectory is considered to be non-reactive. While the diabatic angular momentum does not give us any indication about the final outcome of a trajectory as it is changing rapidly from practically zero to very high values with a frequency that is determined, to a large extent, by the ion–solvent vibrational motion (middle panel of figure 18), there is an effective adiabatic 'solution' angular momentum that one can use (already at $t = 0$ when the trajectory is initiated) to predict the end result. It is important to note that the set of adiabatic coordinates is not the result of thermal averaging which is often employed in the calculation of a rate constant for activationless reactions in solution. Rather, the character of the adiabatic uncoupled set is complicated and it basically involves a substantial mixing between the two original modes. The extent of mixing is determined by the magnitude of the coupling terms, both kinetic and potential.

Before concluding we wish to address the nature and magnitude of the different coupling terms. The extent of kinetic coupling (last term of equation (63)) is determined by the masses and for our choice of similar masses it is relatively large. The potential coupling term, $C(q)$, is relatively small (if it is too large the potential becomes more spherical about the centre of mass and the rotation is frozen) but it plays a major role

in our system as it mimics the reorganization of the solvent. To understand the role of the kinetic coupling it is useful to think of our system as a triatomic molecule, where heavy atom blocking is a known phenomenon (Lederman *et al.* 1989, Uzer and Hynes 1989). When the mass of the central atom (the ion in our model) is increased the degree of mixing between the two modes decreases (i.e., lower coupling) and the use of local modes rather than normal modes is physically more correct. This is true for both the model and the MD simulations. When the mass of the ion increases, the coupling of the ion-molecule vibrational motion to the reaction coordinate is less effective. The small value of the potential energy coupling term need not surprise us as it is well known that for triatomic molecules the experimental results are often recovered quite accurately even if this term is neglected and only the kinetic coupling term is taken into account (Child and Halonen 1985, Henry 1977, Jaffe and Brumer 1980).

7. Concluding remarks

This review discussed aspects of our current understanding of both the kinetics and the dynamics of reactions in solution. By kinetics we mean the study of the rates of chemical reactions starting with thermal reactants. Unlike the situation in the gas phase, where one can select the initial state of the reactants before the collision, this is far less practical in solution. On the other hand, what one can change in solution chemistry, but not in the gas phase, is the nature of the solvent. For both these reasons, the kinetics of reactions is the level at which the theory can meet with much of the available experiments. It is precisely because it is not so readily possible to probe the dynamics that we need to rely more on the theory. A typical example is any activated chemical reaction. In the gas phase, it is necessary that the well separated reactants have sufficient energy to cross the barrier. Otherwise, they will simply fail to react. Not so in solution. The well separated reactants, even if strongly coupled to the solvent, are thermal. Therefore, as the reactants approach one another, the solvent must reorganize so as to provide the energy required to climb the barrier. If there is a surface of no return separating the reactants and products, then transition state theory tells us that the dynamical details of how the solvent does this do not matter, as far as the overall rate is concerned. Still, it is of interest to know what is the mechanism by which the required activation takes place. Is it a slow Brownian-like accumulation of energy or is it a rather impulsive event? In section 5 we suggested that in weakly coupled solvents it is often the latter and that a solvent–solute coupling of almost chemical strength is required for the former. Photochemical initiation of reactions, (particularly unimolecular ones (Whitnell *et al.* 1992)), in solution, clusters (Bormann *et al.*1993, Fei *et al.* 1992, Liu *et al.* 1993, Potter *et al.* 1992) and glasses allows for a real time probing and will be soon providing information that can directly test out understanding of the dynamics of reactions in liquids.

Even at the level of a kinetic description, our understanding is less complete than one might wish. One can always regard the reactants plus a large chunk of the solvent an one supramolecule and compute for it a reaction path leading from reactants to products. Our understanding of potential energy surfaces of many atom systems (e.g., Berry 1991, 1994, Onuchic and Wolynes 1993) leads one to expect that there can be more than one barrier along it. Simulations of reactive events are clearly one way to learn more about what really takes place. Another is the computation of the potential of mean force along possible reaction paths, e.g., Jorgensen (1989). This potential determines the equilibrium rate of the crossing of a dividing surface at any

given point. Of course, at an arbitrary point along the reaction path, it is not the case that all trajectories that cross the dividing surface originated from the reactants. Nor will they all proceed to form products. If there are distinct barriers along the way then the analysis of section 3.3. shows how one can combine such crossing rates so as to obtain the net reaction rate.

In transition state theory we take it that there is one location where the crossing is rate determining. Even then things have not simplified enough. For what we really want are answers like what is the role of the solvent in determining the reaction rate. But the theory is cast in terms of the partition function of the supramolecule evaluated at the transition state configuration. An exact answer is to evaluate the potential of mean force at that location. Typically this is a numerically intensive task and so does not provide ready insight. There are essentially three practical alternatives. The first is to relate the partition function to other thermodynamic quantities for which one can develop an intuition (in the case of the transition state) or which can be measured (in the case of the reactants). The other two possible routes require a factorization of the partition function. Such a factorization necessarily implies additivity of the relevant energies and so, since the solvent and solute interact, this means that it is the properties of both solvent and solute that have to jointly enter the final answer. The two alternatives correspond to the two possible routes available for computing a partition function. One is the evaluation of a phase space integral or, in quantum mechanics, as a sum over states. The integrand (or summand) is the Boltzmann factor. If the energy can be expressed as a sum of terms, the Boltzmann factor factorizes and so does the partition function. This route is best when it is possible to account for the solvent–solute coupling as an additional term in the energy which is not dependent on either the solvent or the solute coordinates. The free volume correction, sections 2.1. and 3.1., provides the simplest illustration of this approach. The other alternative is to factorize the partition function as a momentum integral times a coordinate (or configurational) integral. The Boltzmann factor in the configuration integral is given in terms of the potential energy of the system. Hence this alternative is more practical if a good understanding of the solvent–solute coupling is available. What one now has to implement is a sequential factorization of the configurational integral. The use of local coordinates for doing this has been discussed in section 2.2.

Molecular dynamics simulations for reactions in solution are currently limited primarily by our very incomplete understanding of potentials in many-atom systems. For an assumed potential one can quite readily integrate the equations of motion over the time interval required for a barrier ascent and descent, retaining a realistic number of solvent shells about the reactants, even for a solvent with internal structure. The reason why this is practical is the rather short-time interval that is involved (see figure 6). This is also the reason why direct reaction dynamics will be the same in clusters, liquids and glasses. (The one advantage of either the clusters or the glass is that they provide for the possibility of a non-equilibrium environment for the reactants.) The study of the dynamics is less amenable to a direct computational approach if long-term caging takes place. One can then however use the discussion of section 3.3. to limit the actual dynamical computation to the process of barrier crossing itself. Methods for treating systems with different time-scales are also being developed (Tuckerman *et al.* 1992). Much current research interest is focused on processes which take place on more than one potential energy surface (Makarov and Makri 1993, Wolynes 1987).

As in the gas phase (Levine and Bernstein 1987) the computational study of

dynamics can be complemented by the introduction of more intuitive models. In this review we have emphasized a molecular picture rather than incorporating the role of the solvent in frictional terms. In principle this is a matter of convenience but in practice the two alternatives tend to emphasize different aspects. The very finite number of activating/deactivating collisions which take place at the foothills of the barrier to reaction (section 3.3.), the separation of time-scales that one can often identify (section 5.8.), the understanding of steric aspects (Benjamin *et al.* 1990b, Ben-Nun and Levine 1992a) are all readily cast in mechanical terms and thereby fall within the same framework which has been successful in the gas phase and is currently being applied to reactions in clusters and in solution.

Acknowledgments

MBN is a Clore Foundation scholar. This work was supported by the U.S.–Israel Binational Science Foundation (BSF), Jerusalem, Israel, and by the Stiftung Volkswagenwerk. The Fritz Haber Research Center is supported by the Minerva Gesellschaft für die Forschung, mbH, Munich, Germany.

References

ADAMS, N. G., SMITH, D., and FERGUSON, E. E., 1983, *Int. J. Mass Spectrum. Ion. Proc.*, **67,** 67.
ADELMAN, S. A., 1983, *Adv. chem. Phys.*, **53,** 61; 1987, *Rev. chem. Int.*, **8,** 321.
AGMON, N., and LEVINE, R. D., 1993, *Chem. Phys. Lett.*, **206,** 143; 1994, editors, *Chem. Phys.*, **183** (2,3).
AMAR, F. G., and PERARA, L., 1991, *Z. Phys.* D, **20,** 173.
ANDERSON, J. B., 1973, *J. chem. Phys.*, **58,** 4684: 1975, *Ibid.*, **62,** 2446.
BAGCHI, B., 1989, *Ann. Rev. Phys. Chem.*, **40,** 115.
BAGCHI, B., and FLEMING, G. R., 1990, *J. phys. Chem.*, **94,** 9.
BANIN, U., WALDMAN, A., and RUHMAN, S., 1992, *J. chem. Phys.*, **96,** 2416.
BANIN, U., and RUHMAN, S., 1993, *J. chem. Phys.*, **98,** 4391.
BARLOW, S. E., VAN DOREN, J. M., ROWE, B. R., MARQUETTE, J. B., DUPERRAT, G., and DURUP-FERGUSON, M. J., 1986, *Chem. Phys.*, **85,** 3851.
BASILEVSKY, M. V., and RYABOV, V. M., 1982, *Adv. quant. Chem.*, **15,** 1.
BEN-AMOTZ, D., and HARRIS, C. B., 1987, *J. chem. Phys.*, **86,** 5433.
BEN-NAIM, A., 1974, *Water and Aqueous Solutions* (New York: Plenum Press).
BEN-NUN, M., and LEVINE, R. D., 1992a, *J. phys. Chem.*, **96,** 1523; 1992b, *J. chem. Phys.*, **97,** 8341; 1993a, *J. phys. Chem.*, **97,** 2334; 1993b, *Chem. Phys. Lett.*, **203,** 450; 1993c, *Ibid.*, **214,** 175; 1994, *J. chem. Phys.*, **100,** 3594.
BENJAMIN, I., GERTNER, B. J., TANG, N. J., and WILSON, K. R., 1990a, *J. Am. chem. Soc.*, **112,** 524.
BENJAMIN, I., LEE, L. L., LI, Y. S., and WILSON, K. R., 1991, *Chem. Phys.*, **152,** 1.
BENJAMIN, I., LIU, A., WILSON, K. R., and LEVINE, R. D., 1990b, *J. phys. Chem.*, **94,** 3937.
BENJAMIN, I., and WHITNELL, R. M., 1993, *Chem. Phys. Lett.*, **204,** 45.
BENNETT, C. H., 1977, *Algorithms for Chemical Computations*, edited by R. E. Christoffersen (Washington: ACS).
BENSON, S. W., 1960, *The Foundations of Chemical Kinetics* (New York: McGraw-Hill).
BERGSMA, J. P., REIMER, J. R., WILSON, K. R., and HYNES, J. T., 1986, *J. chem. Phys.*, **85,** 5625.
BERNE, B. J., BORKOVEC, M., and STRAUB, J. E., 1988, *J. phys. Chem.*, **92,** 3711.
BERRY, R. S., 1991, *Mode Selective Chemistry*, edited by J. Jortner, A. Pullman and R. D. Levine (Dordrecht: Kluwer), p. 1; 1994, *J. phys. Chem.*, **98,** 6910.
BJERRUM, N., 1914, *Verhandl. deut. Physik. Ges.*, **16,** 737.
BORKOVEC, M., and BERNE, B. J., 1986, *J. chem. Phys.*, **84,** 4327.
BORRMANN, A., LI, Z., and MARTENS, C. C., 1993, *J. chem. Phys.*, **98,** 8514.
BURSHTEIN, A., and KIVELSON, D., 1991, editors, *Chem. Phys.*, **152** (1,2).
CALDEIRA, A. O., and LEGGETT, A. J., 1983a, *Ann. Phys.*, **149,** 374: 1983b, *Physica* A, **121,** 587.
CHANDLER, D., 1986, *J. statist. Phys.*, **42,** 49; 1990, *J. Phys.* C, **2,** SA13.

CHARUTZ, D. M., and LEVINE, R. D., 1991a, *Chem. Phys.*, **152,** 31; 1991b, *Phys. Rev. Lett.*, **66,** 1251; 1992, *Chem. Phys.*, **152,** 321; 1993, *J. chem. Phys.*, **98,** 1979.
CHESNOY, J., and GALE, G. M., 1988, *Adv. chem. Phys.*, **70,** 297.
CHILD, M. S., and HALONEN, L., 1985, *Adv. chem. Phys.*, **57,** 1.
CICCOTTI, G., FERRARIO, M., HYNES, J. T., and KAPRAL, R., 1990, *J. chem. Phys.*, **93,** 7137.
CLARK, I. D., and WAYNE, R. P., 1969, *Comprehensive Chemical Kinetics*, Vol. 2, edited by C. H. Bamford and C. F. H. Tipper (Amsterdam: Elsevier Publishing Company), chap. 4.
CLARY, D. C., 1990, *Ann. Rev. phys. Chem.*, **41,** 61.
DACK, M. R. J., 1974, *J. chem. Ed.*, **51,** 231.
DANTUS, M., BOWMAN, R. M., GRUBEL, M., and ZEWAIL, A. H., 1989, *J. chem. Phys.*, **91,** 7437.
ECO, U., 1994, *How to Travel with a Salmon* (New York: Harcourt Brace).
ELEY, D. D., 1939, *Trans. Faraday Soc.*, **35,** 1281.
EVANS, M. G., and POLANYI, M., 1935, *Trans. Faraday Soc.*, **31,** 875; 1937, *Ibid.*, **33,** 448.
EWING, G., 1978, *Chem. Phys.*, **29,** 253.
EYRING, H., and HIRSCHFELDER, J. O., 1937, *J. phys. Chem.*, **41,** 249.
EYRING, H., HIRSCHFELDER, J. O., and TAYLOR, H. S., 1936, *J. chem. Phys.*, **4,** 479.
FEI, S., ZHENG, X., HEAVEN, M. C., and TELLINGHUISEN, J., 1992, *J. chem. Phys.*, **97,** 6057.
FERGUSON, E. E., 1974, *Rev. Geophys. Space Phys.*, **12,** 703.
FISCHER, S. F., and RATNER, M. A., 1972, *J. chem. Phys.*, **57,** 2769.
FLEMING, G. R., and WOLYNES, P. G., 1990, *Phys. Today*, May, 36.
FONSECA, T., GOMES, J. A. N. F., GRIGOLINI, P., and MARCHESONI, F., 1985, *Adv. chem. Phys.*, **62,** 389.
FOWLER, R. H., and GUGGENHEIM, E. A., 1939, *Statistical Thermodynamics* (Cambridge University Press).
FRANK, J., and RABINOWITCH, E., 1934, *Trans. Faraday Soc.*, **30,** 120.
GERTNER, B. J., BERGSMA, J. P., WILSON, K. R., LEE, S., and HYNES, J. T., 1987, *J. chem. Phys.*, **86,** 1377.
GERTNER, B. J., BERGSMA, J. P., WILSON K. R., and HYNES, J. T., 1989, *J. chem. Phys.*, **90,** 3537.
GERTNER, B. J., WHITNELL, R. M., WILSON, K. R., and HYNES, J. T., 1991, *J. Am. chem. Soc.*, **113,** 74.
GIOUMOUSIS, G., and STEVENSON, D. P., 1958, *J. chem. Phys.*, **29,** 294.
GLASSTONE, S., LAIDLER, K. J., and EYRING, H., 1941, *The Theory of Rate Processes* (New York: McGraw-Hill).
GORIN, E., 1938, *Acta Physichim U.R.S.S.*, **9,** 691.
GRAENER, H., YE, T. Q., and LAUBEREAU, A., 1989, *J. chem. Phys.*, **91,** 1043.
GROTE, R. F., and HYNES, J. T., 1980, *J. chem. Phys.*, **91,** 1043.
HÄNGGI, P., TALKNER, P., and BORKOVEC, M., 1990, *Rev. mod. Phys.*, **62,** 251.
HARRIS, A. L., BROWN, J. K., and HARRIS, C. B., 1988, *Ann. Rev. phys. Chem.*, **39,** 341.
HARRIS, C. B., SMITH, D. E., and RUSSELL, D. J., 1990, *Chem. Rev.*, **90,** 481.
HASE, W. L., DARLING, C. L., and ZHU, L., 1992, *J. chem. Phys.*, **96,** 8295.
HAYNES, G. R., VOTH, G. A., and POLLAK, E., 1993, *Chem. Phys. Lett.*, **207,** 309.
HENRY, B. R., 1977, *Accts. chem. Res.*, **10,** 207.
HERSCHBACH, D. R., JOHNSTON, H. S., and RAPP, D., 1959, *J. chem. Phys.*, **31,** 1652.
HILDEBRAND, J. H., 1929, *J. Am. chem. Soc.*, **51,** 66.
HILDEBRAND, J. H., and SCOTT, R. L., 1962, *Regular Solutions* (Englewood Cliffs, New Jersey: Prentice Hall).
HILDEBRAND, J. H., and WOOD, S. E., 1933, *J. chem. Phys.*, **1,** 817.
HILL, T. L., 1987, *Statistical Mechanics Principles and Selected Applications* (New York: Dover).
HIRSCHFELDER, J. O., 1939, *J. chem. Ed.*, **16,** 540.
HIRSCHFELDER, J. O., CURTISS, C. F., and BIRD, R. B., 1954, *Molecular Theory of Gases and Liquids* (New York: John Wiley).
HIRSCHFELDER, J. O., STEVENSON, D., and EYRING, H., 1937, *J. chem. Phys.*, **5,** 896.
HIRSCHFELDER, J. O., and WIGNER, E., 1939, *J. chem. Phys.*, **7,** 616.
HOFACKER, G. L., 1963, *Z. Naturforsch* a, **18,** 607.
HOFACKER, G. L., and LEVINE, R. D., 1971, *Chem. Phys. Lett.*, **9,** 617.
HOHN, F. E., 1973, *Elementary Matrix Algebra* (New York: Macmillan Company).

HYNES, J. T., 1985a, *Ann. Rev. phys. Chem.*, **36,** 573; 1985b, *The Theory of Chemical Reaction Dynamics*, Vol. 4, edited by M. Baer (Boca Raton: CRC).
ISAACS, N. S., 1981, *Liquid Phase High Pressure Chemistry* (New York: Wiley).
JAFFE, C., and BRUMER, P., 1980, *J. chem. Phys.*, **73,** 5646.
JENSEN, F., 1992, *Chem. Phys. Lett.*, **196,** 368.
JOHNSTON, H. S., 1966, *Gas Phase Reaction Rate Theory* (New York; the Ronald Press Company).
JORGENSEN, W. L., 1988, *Adv. chem. Phys.*, **70,** 469.
JORTNER, J., PULLMAN, B., and LEVINE, R. D. (editors), 1993, *Reaction Dynamics in Clusters and Condensed Phases* (Dordrecht: Reidel).
KECK, J. C., 1962, *Discuss. Faraday Soc.*, **33,** 73; 1967, *Adv. Chem. Phys.*, **13,** 85.
KEIRSTEAD, W. P., WILSON, K. R., and HYNES, J. T., 1991, *J. chem. Phys.*, **95,** 5256.
KHUNDKAR, L. R., and ZEWAIL, A. H., 1990, *Ann. Rev. phys. Chem.*, **41,** 15.
KIRKWOOD, J. G., 1950, *J. chem. Phys.*, **18,** 380.
KÖRÖSY, F., 1937, *Trans. Faraday Soc.*, **33,** 416.
KOSZYKOWSKI, M. L., NOID, D. W., and MARCUS, R. A., 1982, *J. phys. Chem.*, **86,** 2113.
KRAMERS, H. A., 1940, *Physica* A, **7,** 284.
KRISHAN, R., SINGH, S., and ROBINSON, G. W., 1992a, *J. chem. Phys.*, **97,** 5516; 1992b, *Phys. Rev.* A, **45,** 5408.
LAUBEREAU, A., and KAISER, W., 1978, *Rev. mod. Phys.*, **50,** 607.
LAX, M., 1952, *J. chem. Phys.*, **20,** 1752.
LEDERMAN, L., LOPEZ, V., FAIRMAN, V., VOTH, G. A., and MARCUS, R. A., 1989, *Chem. Phys.*, **139,** 171.
LEVINE, R. D., 1990, *Chem. Phys. Lett.*, **175,** 331.
LEVINE, R. D., and BERNSTEIN, R. B., 1987, *Molecular Reaction Dynamics and Chemical Reactivity* (Oxford University Press); 1988, *J. phys. Chem.*, **92,** 6954.
LI, Y. S., and WILSON, K. R., 1990, *J. chem. Phys.*, **93,** 8821.
LIFSHITZ, C., LOUAGE, F., AVIYENTE, V., and SONG, K., 1991, *J. phys. Chem.*, **95,** 9298.
LIM, K. F., and BRAUMAN, J. I., 1991, *J. chem. Phys.*, **94,** 7164.
LIU, Q., WANG, J. K., and ZEWAIL, A. H., 1993, *Nature*, **364,** 427.
MAKAROV, D. E., and MAKRI, N., 1993, *Phys. Rev.* A, **48,** 3626.
MARCUS, R. A., 1966, *J. chem. Phys.*, **45,** 4493.
MAYER, J. E., and MAYER, M. G., 1940, *Statistical Mechanics* (New York: John Wiley and Sons, Inc.), pp. 213–217.
MCMANIS, G. E., GOCHEV, A., and WEAVER, M. J., 1991, *Chem. Phys.*, **152,** 107.
MELNIKOV, V. I., 1991, *Phys. Rep.*, **209,** 1.
MILLER, W. H., 1976, *J. chem. Phys.*, **65,** 2216; 1983, *Ibid.*, **87,** 3811.
MOKHTARI, A., CHEBIRA, A., and CHESNOY, J., 1990, *J. Am. Opt. Soc.* B, **7,** 1551.
NELSON, K. A., and WILLIAMS, L. R., 1987, *Phys. Rev. Lett.*, **58,** 745.
NERIA, E., and NITZAN, A., 1992, *J. Chem. Phys.*, **96,** 5433; **1994,** *Ibid.*, **100,** 3855.
NITZAN, A., 1988, *Adv. chem. Phys.*, **70,** 489.
NORTH, A. M., 1964, *The Theory of Chemical Reactions in Liquids* (London: Methuen).
NOYES, R. M., 1961, *Progress in Reaction Kinetics*, Vol. 1, edited by G. Porter (Oxford: Pergamon), p. 129.
OLMTEAD, W. N., and BRAUMAN, J. I., 1977, *J. Am. chem. Soc.*, **99,** 4219.
ONUCHIC, J. N., and WOLYNES, P. G., 1993, *J. chem. Phys.*, **98,** 2218.
OXTOBY, D. W., 1981, *Adv. chem. Phys.*, **47,** 487.
PAPANIKOLAS, J. M., GORD, J. R., LEVINGER, N. E., RAY, D., VORSA, V., and LINEBERGER, W. C., 1991, *J. phys. Chem.*, **95,** 8028.
PAPANIKOLAS, J. M., VORSA, V., NADAL, M. E., CAMPAGNOLA, P. J., GORD, J. R., and LINEBERGER, W. C., 1992, *J. chem. Phys.*, **97,** 7002.
PAPOULIS, A., 1962, *The Fourier Integral and Its Applications* (New York; McGraw-Hill).
PATRON, F., and ADELMAN, S. A., 1991, *J. chem. Phys.*, **152,** 121.
PELLERITE, M. J., and BRAUMAN, J. I., 1980, *J. Am. phys. Soc.*, **102,** 5593.
PERARA, L., and AMAR, F. G., 1989, *J. chem. Phys.*, **90,** 7354.
POLLAK, E., 1986a, *J. chem. Phys.*, **85,** 865; 1986b, *Phys. Rev.* A, **33,** 4244; 1987, *J. chem. Phys.*, **86,** 3944.
POLLARD, W. T., and MATHIES, R. A., 1992, *Ann. Rev. phys. Chem.*, **43,** 497.

POTTER, E. D., LIU, Q., and ZEWAIL, A. H., 1992, *Chem. Phys. Lett.*, **200,** 605.
RABANI, E., CHARUTZ, D. M., and LEVINE, R. D., 1991, *J. phys. Chem.*, **95,** 10551.
REY, R., and GUÀRDIA, E., 1992, *J. phys. Chem.*, **96,** 4712.
REBENTROST, F., 1981, *Theoretical Chemistry; Theory of Scattering*, Vol. 6B (New York: Academic).
ROBINSON, G. W., SINGH, S., KRISHNAN, R., ZHU, S. B., and LEE, J., 1990, *J. Phys. Chem.*, **94,** 4.
ROSKER, M. J., ROSE, R. S., and ZEWAIL, A. H., 1988, *Chem. Phys. Lett.*, **152,** 7.
SCEATS, M. G., 1986, *Chem. Phys. Lett.*, **128,** 55.
SCHERER, N. F., JONAS, D. M., and FLEMING, G. R., 1993, *J. Chem. Phys.*, **99,** 153.
SCHROEDER, J., and TROE, J., 1987, *Ann. Rev. phys. Chem.*, **38,** 163.
SEELEY, G., and KEYES, T., 1989, *J. chem. Phys.*, **91,** 5581.
SMITH, D. E., and HARRIS, C. B., 1990, *J. chem. Phys.*, **92,** 1304.
SMITH, I. W. M., 1980, *Kinetics and Dynamics of Elementary Gas Phase Reactions* (London: Butterworths).
SMITH., S. C., MCEWAN, M. J., and GILBERT, R. G., 1989, *J. phys. Chem.*, **93,** 8142.
STAIB, A., and HYNES, J. T., 1993, *Chem. Phys. Lett.*, **204,** 197.
STILLINGER, F. H., and WEBER, T. A., 1984a, *Science*, **225,** 983; 1984b, *J. chem. Phys.*, **80,** 4434.
STRAUB, J. E., BORKOVEC, M., and BERNE, B. J., 1986, *J. chem. Phys.*, **84,** 1788.
STRAUS, J. B., LLORENTA, J. B., and VOTH, G. A., 1993, *J. chem. Phys.*, **98,** 4082.
TALKNER, P., and BRAUN, H. B., 1988, *J. chem. Phys.*, **88,** 7537.
TARJUS, G., and KIVELSON, D., 1991, *Chem. Phys.*, **152,** 153.
TROE, J., 1986, *J. phys. Chem.*, **90,** 357; 1987, *Int. J. Mass Spectrum. Ion Proc.*, **80,** 17; 1989, *Z. phys. Chem.*, **161,** 209.
TRUHLAR, D. G., 1990, *J. Am. chem. Soc.*, **112,** 3347.
TUCKER, S. C., 1993, *J. phys. Chem.*, **97,** 1596.
TUCKER, S. C., and TRUHLAR, D. G., 1989, *J. phys. Chem.*, **93,** 8138.
TUCKER, S. C., TUCKERMAN, M. E., BERNE, B. J., and POLLAK, E., 1991, *J. chem. Phys.*, **95,** 5809.
TUCKERMAN, M., BERNE, B. J., and MARTYNA, G. J., 1992, *J. chem. Phys.*, **97,** 1990.
TURULSKI, J., and NIEDZIELSKY, J., 1988, *J. Chem. Soc. Faraday Trans.*, **84,** 347.
UHLIG, H. H., 1937, *J. phys. Chem.*, **41,** 1215.
UZER, T., and HYNES, J. T., 1989, *Chem. Phys.*, **139,** 163.
VAN DER ZWAN, G., and HYNES, J. T., 1982, *J. chem. Phys.*, **76,** 2993; 1983, *Ibid.*, **78,** 4174; 1984, *Ibid.*, **90,** 21.
VANDE, L., and HASE, W. L., 1990, *J. phys. Chem.*, **94,** 2778.
VOTH, G. A., 1992, *J. chem. Phys.*, **97,** 5908.
WAN, Y., and STRATT, R. M., 1994, *J. chem. Phys.*, **100,** 5123.
WESTON, R. JR., and SCHWARTZ, H. A., 1972, *Chemical Kinetics* (Englewood Cliffs, New Jersey: Prentice-Hall, Inc.).
WHITNELL, R. M., and WILSON, K. R., 1993, *Reviews in Computational Chemistry*, Vol. 6, edited by K. B., Lopkowitz and D. B. Boyd (New York: VCH).
WILSON, E. B. JR., DECIUS, J. C., and CROSS, P. C., 1954, *Molecular Vibrations* (New York; McGraw-Hill).
WILSON, K. R., 1988, *Chemical Reactivity in Liquids; Fundamental Aspects*, edited by M. Moreau and P. Turk (New York: Plenum).
WILSON, K. R., and LEVINE, R. D., 1988, *Chem. Phys. Lett.*, **152,** 435.
WINSTEIN, S., CLIPPINGER, E., FAINBAR, A. H., and ROBINSON, G. C., 1954, *J. Am. chem. Soc.*, **76,** 259.
WISE, F. M., ROSKER, M. J., and TANG, C. L., 1987, *J. chem. Phys.*, **86,** 2827.
WOLYNES, P. J., 1987, *J. chem. Phys.*, **86,** 1957.
YAN, Y., WHITNELL, R. M., WILSON, K. R., and ZEWAIL, A. H., 1992, *Chem. Phys. Lett.*, **193,** 402.
ZADOYAN, R., LI, Z., ASHJIAN, P., MARTENS, C. C., and APKARIAN, V. A., 1994, *Chem. Phys. Lett.*, **218,** 504.
ZEWAIL, A. H., 1991, *Discuss. Faraday Soc.*, **91,** 207.
ZHANG, J. Z., and HARRIS, C. B., 1991, *J. chem. Phys.*, **94,** 5586.
ZOVAL, J., and APKARIAN, V. A., 1994, *J. phys. Chem.*, **98,** 7945.
ZWANZIG, R., 1987, *J. chem. Phys.*, **86,** 5801.